

AD-A095 269

NAVAL SURFACE WEAPONS CENTER DAHLGREN VA
THE INFLUENCE OF ROLL ORIENTATION-DEPENDENT AERODYNAMICS ON THE--ETC(U)

F/G 20/4

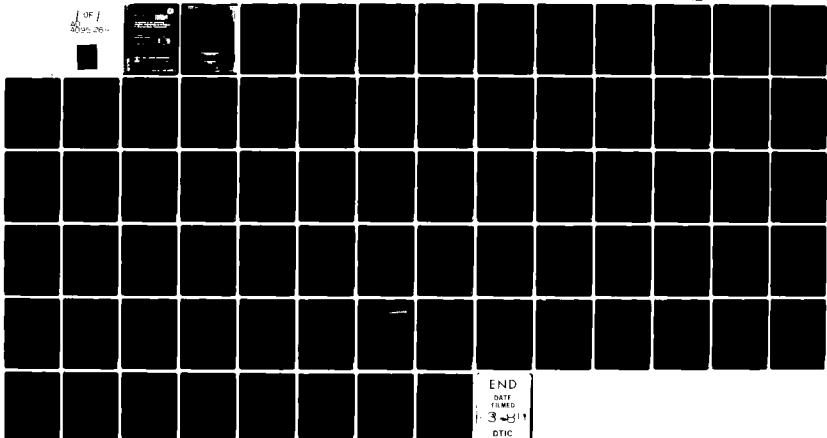
JAN 81 T R PEPITONE

UNCLASSIFIED

NSWC-TR-79-416

NL

1 of 1
00000000



END
DATE
FILMED
3-5-11
DTIC

AD A095269



UNCLASSIFIED

SECURITY CLASSIFICATION OF THIS PAGE (When Data Entered)

REPORT DOCUMENTATION PAGE		READ INSTRUCTIONS BEFORE COMPLETING FORM
1. REPORT NUMBER (14) NSWC/TR-79-416	2. GOVT ACCESSION NO. (16) AD-A095	3. RECIPIENT'S CATALOG NUMBER 269
4. TITLE (and Subtitle) (6) THE INFLUENCE OF ROLL ORIENTATION-DEPENDENT AERODYNAMICS ON THE STABILITY OF CRUCIFORM MISSILE CONFIGURATIONS.		5. TYPE OF REPORT & PERIOD COVERED (9) Final R & F T.O.
7. AUTHOR(s) (10) T. R. PEPITONE		6. PERFORMING ORG. REPORT NUMBER
9. PERFORMING ORGANIZATION NAME AND ADDRESS Naval Surface Weapons Center (K21) Dahlgren, Virginia 22448		8. CONTRACT OR GRANT NUMBER(s) (12) 766
11. CONTROLLING OFFICE NAME AND ADDRESS Naval Weapons Center China Lake, CA 93555		10. PROGRAM ELEMENT, PROJECT, TASK AREA & WORK UNIT NUMBERS NIF, 62332N, (16) AF32395
14. MONITORING AGENCY NAME & ADDRESS (if different from Controlling Office)		12. REPORT DATE January 1981
		13. NUMBER OF PAGES 74
		15. SECURITY CLASS. (of this report) Unclassified
		15a. DECLASSIFICATION/DOWNGRADING SCHEDULE
16. DISTRIBUTION STATEMENT (of this Report) Approved for public release; distribution unlimited.		
17. DISTRIBUTION STATEMENT (of the abstract entered in Block 20, if different from Report)		
18. SUPPLEMENTARY NOTES		
19. KEY WORDS (Continue on reverse side if necessary and identify by block number)		
20. ABSTRACT (Continue on reverse side if necessary and identify by block number) The angular motion of a symmetric, cruciform missile, having roll orientation-dependent aerodynamics, is studied. An aerodynamic moment expansion, consistent with rotational and reflectional symmetry arguments, is incorporated into the equations of missile angular motion. A generalized version of the method of multiple scales is incorporated to generate approximate solutions to the equations of angular motion for three specific cases: free-flight angular motion at constant		

DD FORMS 1473
1 JAN 73

EDITION OF 1 NOV 65 IS OBSOLETE
S/N 0192-014-6601

UNCLASSIFIED

SECURITY CLASSIFICATION OF THIS PAGE (When Data Entered)

567

UNCLASSIFIED

SECURITY CLASSIFICATION OF THIS PAGE (When Data Entered)

20. Abstract (Continued)

cont.

roll rate, induced rolling motion with a priori yawing motion, and finally the combined problem of coupled yawing and rolling motion. Critical roll rates are identified and solutions valid in the vicinity of these singular conditions are generated. Approximate solutions used to derive stability criteria are compared with numerical solutions of exact, nonlinear equations of motion. Results of the perturbation solutions show good agreement with the exact calculations for moderate angles of attack.



UNCLASSIFIED

SECURITY CLASSIFICATION OF THIS PAGE (When Data Entered)

FOREWORD

This report describes work directed towards obtaining a better understanding of free-flight, air-launched weapon dynamics.

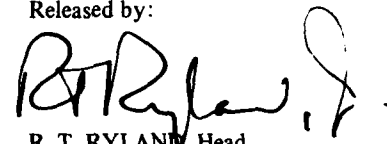
This work was performed under AIRTASK WF 32-395-62332N.

Acknowledgement is due to Mr. W. C. Volz of the Naval Air Systems Command, whose direction and support made the work possible.

This report was reviewed by Dr. F. G. Moore, Head, Aeromechanics Branch and by Mr. C. A. Fisher, Head, Weapon Dynamics Division.

Accession For	
NTIS GRA&I	<input checked="" type="checkbox"/>
DTIC TAB	<input type="checkbox"/>
Unannounced	<input type="checkbox"/>
Justification	
By _____	
Distribution/	
Availability Codes	
Avail and/or	
Dist	Special
A	

Released by:



R. T. RYLAND, Head
Strategic Systems Department

CONTENTS

CHAPTER I – INTRODUCTION	1
CHAPTER II – EQUATIONS OF MOTION AND AERODYNAMIC MOMENT EXPANSIONS	2
A. Equations of Transverse Angular Motion	2
B. Aerodynamic Force and Moment Expansions	4
C. Dynamics and Aerodynamics of Rolling Motion	8
CHAPTER III – ANGULAR MOTION WITH PRESCRIBED ROLLING MOTION	11
A. Nonresonant Solutions	11
B. Resonant Spin	15
CHAPTER IV – INDUCED ROLLING MOTION WITH PRESCRIBED YAWING MOTION	20
A. Nonresonant Solutions	21
B. Resonant Solutions	23
CHAPTER V – COMBINED ROLL-YAW INTERACTION	35
A. Nonresonant Solutions	36
B. Resonant Solutions	38
C. Stability at Resonance	40
CHAPTER VI – SUMMARY AND CONCLUSIONS	53
REFERENCES	54
APPENDIX A – MAPLE-SYNGE THEORY	A-1

NOMENCLATURE

- A Missile reference area, cm^2 .
- C_ℓ Total missile roll moment coefficient.
- C_{ℓ_0} Static roll driving moment coefficient.
- C_{ℓ_p} Linear roll damping moment coefficient.
- $C_{\ell_{\gamma\delta^4}}$ Induced roll moment coefficient.
- $(C_{\tilde{m}} + iC_{\tilde{n}})$ Complex transverse aerodynamic moment expressed in the non-rolling frame.
- $C_m(\gamma)$ Roll-orientation-dependent restoring moment coefficient.
- C_{m_α} Restoring moment coefficient derivative.
- $C_{m_{\alpha_0}}$ Unmodulated restoring moment coefficient derivative.
- $(C_{m_q} + C_{m_{\dot{\alpha}}})$ Pitch damping coefficient derivative.
- $C_{m_{\gamma\delta}}, C_{m_{\gamma\delta^2}}, C_{m_{\gamma\delta^4}}$ Coefficients of the roll orientation-dependent static moment expansion.
- $C_{m_{p\alpha}}$ Linear magnus moment coefficient derivative.
- $C_N(\gamma)$ Roll orientation-dependent normal force coefficient.
- $C_{N_{\alpha_0}}$ Unmodulated normal force coefficient derivative.
- $C_{N_{\gamma\delta^2}}, C_{N_{\gamma\delta^4}}$ Coefficients of the roll orientation-dependent normal force expansion.
- $C_{SN}(\gamma)$ Roll orientation dependent side-force coefficient.
- $C_{sm}(\gamma)$ Roll orientation-dependent side-moment coefficient.
- $C_{sm_\alpha}(\gamma)$ Roll orientation-dependent side-moment coefficient derivative.
- $C_{sm_{\gamma\delta}}$ Linear, roll orientation-dependent side-moment coefficient derivative.
- $(C_{\tilde{y}} + iC_{\tilde{z}})$ Complex transverse force coefficient expressed in the non-rolling frame.
- d Missile reference diameter, cm.

- H $C_{N_{\alpha_0}} - k_t^{-2}(C_{m_q}^* + C_{m_{\dot{\alpha}}}^*)$.
- I_x, I_y Missile polar and transverse moments of inertia, Kgm-m².
- K_1, K_2 Nutation and precession modal vectors.
- K_{1_0}, K_{2_0} Initial values of the nutation and precession modal vectors.
- k_a Missile axial radius of gyration.
- k_t Missile transverse radius of gyration.
- k_1, k_2 Nutation and precession modal amplitudes.
- m Missile mass, kg.
- P $\frac{pd}{V} \left(\frac{I_x}{I_y} \right)$.
- p Roll rate, rad/sec.
- \bar{p} pd/V .
- $(p, \tilde{q}, \tilde{r})$ Missile angular velocity expressed in non-rolling frame.
- p_{ss} Steady-state roll rate.
- q_{∞} Dynamic pressure, $1/2\rho V^2$.
- R $-k_t^{-2} C_{m_{\gamma\delta^2}}^*$.
- \hat{R} $R/(\omega_1 - \omega_2)$.
- S $\bar{\gamma} k_t^{-2} C_{s_m}^*(\gamma)$.
- S_{γ} $C_{N_{\gamma\delta^2}}^* \left(4 \frac{I_y}{I_x} - 1 \right)$.
- s Nondimensional arclength.
- T $C_{N_{\alpha_0}}^* + k_a^{-2} C_{m_{p\alpha}}^*$.
- T_0 Fast time scale.
- T_2, T_4 Slow time scales.
- t Time, sec.

- (u, \tilde{v}, \tilde{w}) Missile velocity vector expressed in the non-rolling frame.
- V Magnitude of the missile velocity, m/sec.
- (x, y, z) Inertial frame coordinates.
- ($X, Y, Z,$) Missile-fixed coordinate frame.
- ($X, \tilde{Y}, \tilde{Z},$) Missile non-rolling coordinate frame.

GREEK SYMBOLS

- α_T Total angle of attack.
- γ Cross flow orientation relative to cruciform.
- $\bar{\gamma}$ u/V .
- δ Magnitude of the complex angle of attack.
- ϵ Smallness parameter.
- θ_1, θ_2 Nutation and precession mode slowly varying phase.
- λ Detuning parameter.
- $\tilde{\mu}$ Complex transverse angular velocity expressed in the non-rolling frame.
- ξ Complex angle of attack expressed in the missile-fixed frame.
- $\tilde{\xi}$ Complex angle of attack expressed in the non-rolling frame.
- ρ Air density kgm/m^3 .
- ϕ Missile roll orientation.
- ϕ_0 Missile initial roll orientation.
- $\psi_{(s)}$ Total phase of the planar motion amplitude.
- ψ_j Total phase of the j^{th} modal amplitude, k_j .
- $\hat{\psi}$ $\psi_j + \theta_j$
- ω_j Frequency of j^{th} modal amplitude k_j .
- ω_j'' $d\omega_j/dT_2$.

MATHEMATICAL NOTATION

- ()' Denotes differentiation with respect to non-dimensional arclength.
- ($\dot{}$) Denotes differentiation with respect to time.
- ($\bar{}$) Denotes matrix.
- ($\tilde{}$) Denotes quantities expressed in the non-rolling frame.
- ($\bar{}$) Denotes the complex conjugate.
- | | Denotes the magnitude of a complex or vector quantity.
- Im Imaginary part.
- Re Real part.

CHAPTER I

INTRODUCTION

The angular motion of a finned missile has long been the subject of extensive experimental and analytical investigations. Much of this work has been a part of the normal aerodynamic design phases of both guided and unguided missiles. However, all too often, the more serious and ambitious of these investigations are undertaken as a direct result of unexpected flight failures, at the expense of time and resources already invested in the design. In hindsight, these flight instabilities are often found to arise from fundamental inadequacies in the missile design or failure on the part of the designer to recognize an important mechanism of aerodynamic coupling.

One of the most severe types of flight instabilities encountered in the free flight of a finned missile is described by large-amplitude angular motion when the missile rolling velocity is in the vicinity of the missile natural frequency (fundamental resonance). This undesirable behavior has been shown to arise as a result of the aerodynamic coupling which exists between the vehicle axial and transverse aerodynamics. This so-called "roll-yaw coupling" has been responsible for the anomalous behavior of several contemporary configurations and, in some instances, has resulted in unacceptable dispersion levels so as to severely degrade weapon effectiveness.

In spite of the vast amount of literature available on the subject, a complete and thorough understanding of the phenomenon has successfully eluded the flight dynamicist for many years. While there have been significant contributions made in recent years¹⁻⁷ in the form of partial solutions, the problem to date, in three degrees of freedom, remains unsolved.

While previous works have treated the possibility of missile resonant behavior in the vicinity of fundamental resonance, they have all had one basic assumption in common: the existence of a small configurational asymmetry, which acts as a harmonic forcing function and is the cause of the subsequent resonant behavior.

If one considers the resonance phenomenon in a somewhat more general light, it seems plausible that the inherent lack of complete axial symmetry introduced by the presence of the fins has the potential for introducing resonant behavior. Missile transient response, in the presence of roll-orientation-dependent aerodynamics, at a number of critical rolling velocities, is precisely the subject of this report. By an analysis of the yawing motion, with the rolling motion known a priori and vice versa, an understanding of coupling mechanisms introduced by the roll-dependent aerodynamics may be gained.

The general case of the angular motion of a symmetric missile having nonlinear roll orientation-dependent aerodynamics, cubic in angle of attack, and constant roll rate is treated via the method of multiple scales. Using the resulting first-approximate solution, missile transient response is investigated and three critical roll rates are identified at zero spin, resonance, and one-half resonant spin. Plane autonomous system theory is used to exhibit the nature of the motion and its dependence on initial conditions.

The induced rolling motion of a cruciform missile with a-priori yawing motion is then studied, using a generalized version of the method of multiple-time scaling to obtain the conditions for roll entrainment. Solutions are shown to be singular at zero spin, resonance, and one-half resonant spin; and additional solutions valid in the vicinity of these roll rates are generated.

Finally, the full nonlinear problem of combined pitch-yaw-roll motion, with roll orientation-dependent axial and transverse aerodynamics, is studied, with no a priori assumptions regarding the motion. Critical roll rates are identified and useful stability criteria are derived.

CHAPTER II

EQUATIONS OF MOTION AND AERODYNAMIC MOMENT EXPANSIONS

A. EQUATIONS OF TRANSVERSE ANGULAR MOTION

In order to introduce the subject and gain insight into the problem, the equations of motion of a rigid, cruciform, free-flight missile having both aerodynamic and inertial symmetry are presented. In the work that follows, use will be made of three frames of reference: an inertial frame, a missile-fixed system, and the "aeroballistic" or nonrolling system.

The (x, y, z) coordinate system of Figure 1 is an inertial frame, with freestream velocity \vec{V} directed along the x -direction. The missile-fixed frame (X, Y, Z) is an orthogonal system, rigidly attached to the missile, with the X -axis along the longitudinal axis of symmetry, the Y -axis containing a fin, and the Z -axis completing the triad. It is convenient to express the equations of motion in terms of dynamical quantities defined in the "aeroballistic" system, $(X, \tilde{Y}, \tilde{Z})$, which is allowed to pitch and yaw with the missile but does not roll. Transformation of vector quantities between the missile-fixed and nonrolling systems is then completely specified by a rotation about the missile X -axis through the roll angle $\hat{\phi}$ defined by

$$\phi = \int p dt \quad (2.1)$$

where p is the missile roll rate and t , time.

Many excellent developments of the equations of motion of a symmetric missile can be found in the literature and for the sake of brevity will not be repeated here. Instead, the nomenclature and results of Reference 8 will be used in writing the equations of angular motion in the nonrolling coordinate system in terms of the translational $(u, \tilde{v}, \tilde{w})$ and rotational $(p, \tilde{q}, \tilde{r})$ velocity components expressed in that frame. From Reference 8 the exact equations of missile angular motion, with constrained center of gravity may be written*

$$\tilde{\xi}' - i\tilde{\gamma}\tilde{\mu} = C_{\tilde{y}}^+ + iC_{\tilde{z}}^* \quad (2.2)$$

$$\tilde{\mu}' - iP\tilde{\mu} = k_t^{-2}(C_m^* + iC_n^*) \quad (2.3)$$

where the complex angle of attack, $\tilde{\xi}$, and the complex angular velocity, $\tilde{\mu}$, are given by

$$\tilde{\xi} = \frac{\tilde{v} + i\tilde{w}}{V} \quad (2.4)$$

$$\tilde{\mu} = \frac{(\tilde{q} + i\tilde{r})d}{V} \quad (2.5)$$

*Assumptions of constant velocity and the omission of gravity are implicit in the use of Equations (2.2) and (2.3).

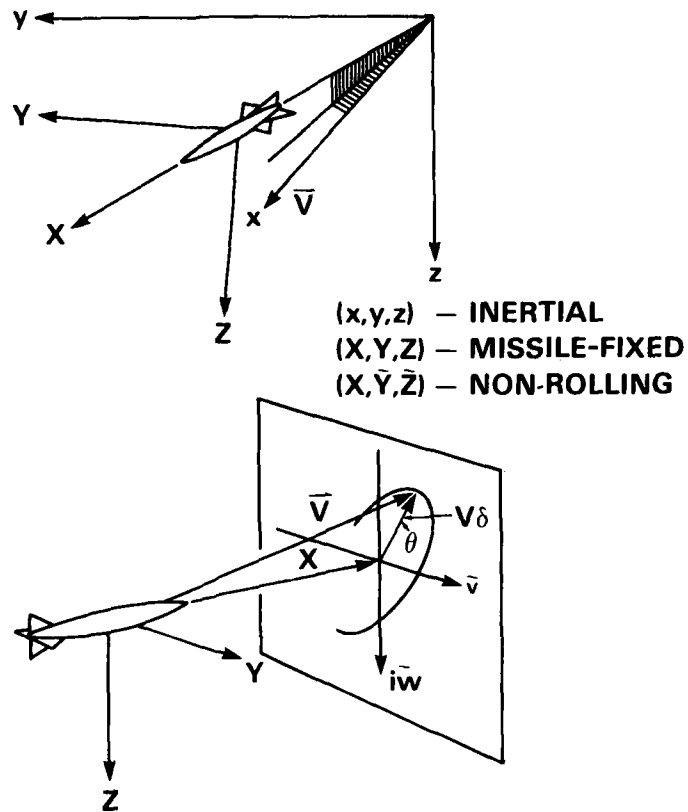


Figure 1. - Coordinate Systems

$$\bar{\gamma} = u/V \quad (2.6)$$

$$P = \frac{\rho d}{V} \frac{I_x}{I_y} \quad (2.7)$$

and

$$k_t^{-2} = \frac{md^2}{I_y} \quad (2.8)$$

In compliance with the methods of Reference 8, the independent variable t has been replaced by the nondimensional arclength, s , defined by

$$s = \int \frac{V}{d} dt \quad (2.9)$$

with $()'$ denoting differentiation with respect to s . The complex moment coefficient in the nonrolling frame $(C_{\bar{m}} + iC_{\bar{n}})$ has been multiplied by the density factor $(\rho Ad/2m)$

$$(C_{\tilde{m}}^* + C_{\tilde{n}}^*) = \frac{\rho A d}{2m} (C_{\tilde{m}} + i C_{\tilde{n}}). \quad (2.10)$$

Now for small angles of attack, the quantity, $\tilde{\gamma}$, is essentially constant at a value of unity since

$$\tilde{\gamma}^2 = 1 - \delta^2 \quad (2.11)$$

where δ represents the magnitude of $\tilde{\xi}$. Therefore, if attention is restricted to small-amplitude motion, the effect of the geometrical nonlinearities $\tilde{\gamma}$ and $\tilde{\gamma}'/\tilde{\gamma}$ may be approximated by⁸

$$\tilde{\gamma} \approx 1 \quad (2.12)$$

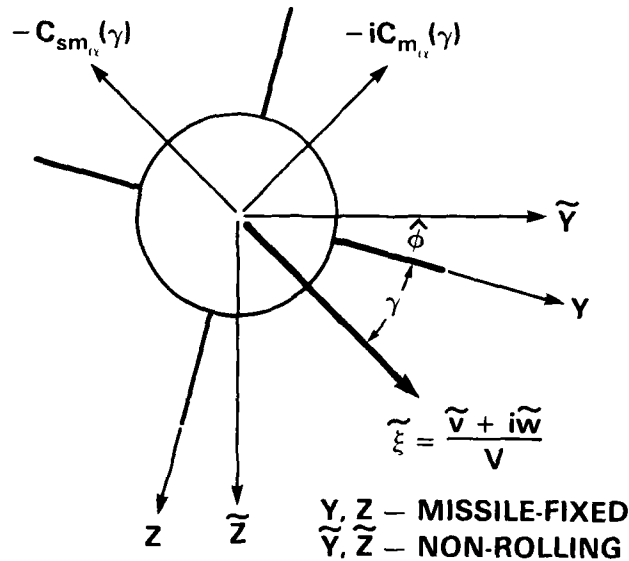
and

$$\tilde{\gamma}'/\tilde{\gamma} \approx 0. \quad (2.13)$$

With the elimination of these geometrical nonlinearities, the only task remaining is a specification of the functional form of the aerodynamics.

B. AERODYNAMIC FORCE AND MOMENT EXPANSIONS

In the case of a cruciform missile, the static restoring moment is not only a function of the angle of attack but is also dependent on the orientation of the plane of the angle of attack relative to the cruciform, as shown in Figure 2. Experimentally, this modulation of the static restoring moment with roll angle is observed to be quite small, for most low-aspect-ratio missile configurations.⁹⁻¹¹ Typical variations of static restoring moment with roll orientation are shown plotted in Figures 3 and 4.



AFT LOOKING FORWARD

Figure 2. Roll-Orientation-Dependent Aerodynamics

In addition to static moment variations, experiment has also shown the existence of a roll-orientation-dependent side moment and its corresponding side force. This "induced" side moment is caused by the lack of complete axial symmetry introduced by the presence of the fins. Thus, when the cross-flow vector impinges on an asymmetric body cross section, at specific roll orientation angles a side-moment arising from this asymmetric pressure distribution results. For typical low-aspect-ratio configurations, wind tunnel tests have shown these side forces and moments to be reasonably approximated by harmonic functions of the roll orientation angle, γ .¹¹ Typical variations of side-force and side-moment with roll orientation are shown in Figures 3 and 4.

Given some rather basic assumptions concerning the origin of the fluid forces acting on a missile possessing n-gonal symmetry, Maple and Syngé¹² have shown that simple rotational and reflectional symmetry considerations can sometimes place unexpected restrictions on the functional form of the missile aerodynamic force and moment system.

The basic hypotheses of the theory are twofold. The first is the aerodynamic hypothesis;¹³ i.e., the aerodynamic forces and moments acting on the missile are completely specified by the instantaneous translational and rotational velocity of the missile relative to the fluid. The second is the assumption that these forces and moments may be represented by a power series expansion in the transverse translational and angular velocity components of the missile. In recent years, the validity of the aerodynamic hypothesis has come under scrutiny, and in some

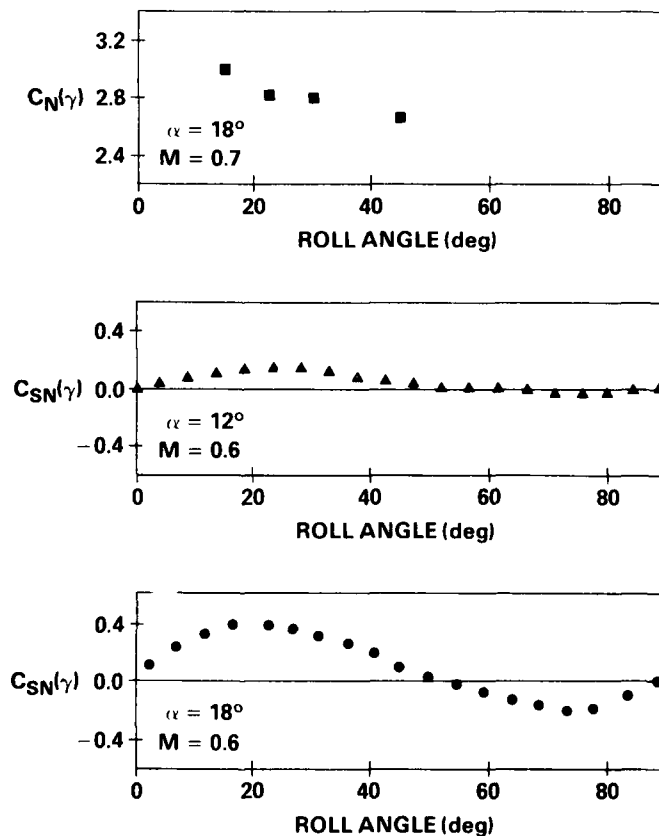


Figure 3. - Typical Restoring Moment and Side Moment Variations with Roll Angle (References 10 and 11)

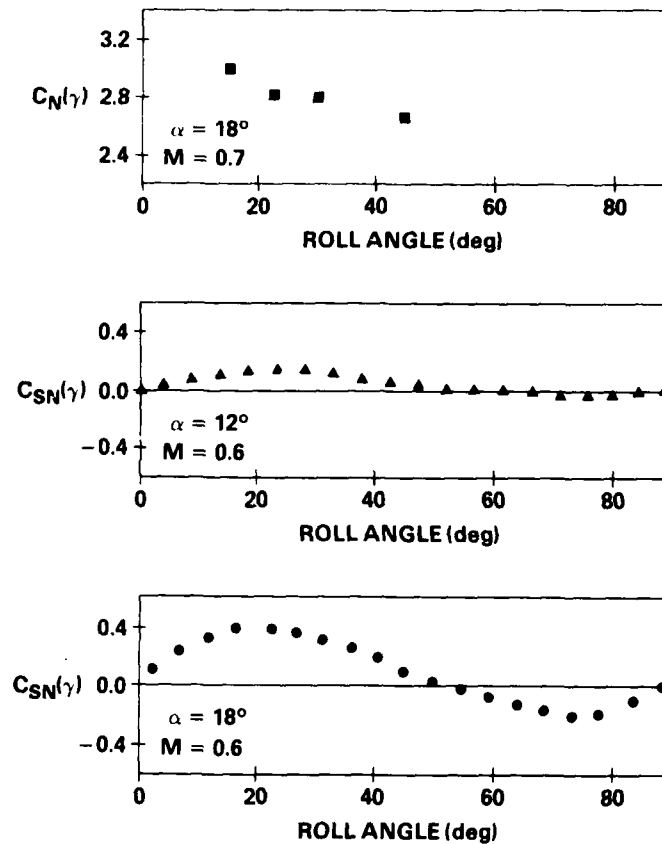


Figure 4. - Typical Normal Force and Side Force Variations with Roll Angle (References 10 and 11)

instances, modifications to the theory have been proposed. Considerations of such mechanisms as nose-generated vorticity and its interaction with the aft body have suggested the possible inclusion of terms that would reflect the recent history of the flow as well as its present state. Nevertheless, over the years, the theory has essentially remained intact, providing the mathematical framework for the basic aerodynamic force and moment expansion.

Only the basic results of the theory are presented herein. A development of the static, roll-orientation-dependent force and moment expansions may be found in the appendix. For a general treatment of the subject, the reader is referred to the original work of Maple and Synge,¹² as well as a somewhat abridged version by Zaroodny.¹⁴

The essence of the method is embodied in the observance of the aerodynamic force and moment expansion under coordinate transformation. The physical reasoning of these operations may be summarized as:

- a. The aerodynamic force and moment expansion, in the nonrolling system, must remain invariant under roll transformations through an angle $2\pi/N$, where N is the number of planes of rotational symmetry (fins).
- b. The aerodynamic force and moment expansions are "antisymmetric" under a reflection of the coordinate system about a plane containing a fin (cruciform missile).

If these operations are performed for a cruciform missile and attention is restricted to the static-roll-orientation-dependent terms of the first harmonic in 4γ , the following force and moment contributions (to fifth order in δ) result:

$$(C_{\tilde{y}} + iC_{\tilde{z}}) = \left[-C_{N_{\alpha_0}} + C_{N_{\gamma\delta^2}}\delta^2 e^{-i4\gamma} + C_{N_{\gamma\delta^4}}\delta^4 e^{i4\gamma} + \dots \right] \tilde{\xi} \quad (2.14)$$

and

$$(C_{\tilde{m}} + C_{\tilde{n}}) = i \left[-C_{m_{\alpha_0}} + C_{m_{\gamma\delta^2}}\delta^2 e^{-i4\gamma} + C_{m_{\gamma\delta^4}}\delta^4 e^{i4\gamma} + \dots \right] \tilde{\xi}. \quad (2.15)$$

Equations (2.14) and (2.15) offer a considerable amount of information concerning the form of the roll-orientation-dependent aerodynamics of a symmetric cruciform missile.

First, it can be seen that the terms linear in angle of attack are free of any γ -dependence. From this fact, it follows that the effects of roll orientation must be limited to terms cubic in the angle of attack and higher. Terms of lower order in δ are incapable of discerning the presence of the fins. Secondly, if Equations (2.14) and (2.15) are expanded into real and imaginary parts, it is seen that for expansions third order in δ and lower, the "in-plane" and "out-of-plane" components due to roll orientation must be equal. For example, the in-plane component of Equation (2.15) is given by

$$C_{m_{in-plane}} = -C_{m_{\alpha_0}} \delta + C_{m_{\gamma\delta^2}} \delta^3 \cos 4\gamma + C_{m_{\gamma\delta^4}} \delta^5 \cos 4\gamma + \dots \quad (2.16)$$

while the out-of-plane component may be written

$$C_{m_{out-of-plane}} = -C_{m_{\gamma\delta^2}} \delta^3 \sin 4\gamma - C_{m_{\gamma\delta^4}} \delta^5 \sin 4\gamma + \dots \quad (2.17)$$

It is easily seen that descriptions of the roll orientation-dependent static moment, up to third order in δ , must have the side moment and modulation component of the restoring moment equal in magnitude.

In the study of roll orientation-dependent forces and moments that follows, terms up to third order in δ and harmonic in 4γ will be retained.

With the static-roll-orientation-dependent forces and moments defined, inclusion of aerodynamic damping ($C_{m_q} + C_{m_{\dot{\alpha}}}$), and a linear magnus moment, $C_{m_{p\alpha}}$, results in the total aerodynamic force and moment system to be considered.

$$(C_{\tilde{y}}^* + iC_{\tilde{z}}^*) = \left[-C_{N_{\alpha_0}}^* + C_{N_{\gamma\delta^2}}^* \delta^2 e^{-i4\gamma} \right] \tilde{\xi} \quad (2.18)$$

$$(C_{\tilde{m}}^* + iC_{\tilde{n}}^*) = \left[-iC_{m_{\alpha_0}}^* + iC_{m_{\gamma\delta^2}}^* \delta^2 e^{-i4\gamma} + C_{m_{p\alpha}}^* \bar{p} \right] \tilde{\xi} - iC_{m_{\dot{\alpha}}}^* \tilde{\xi}' + C_{m_q}^* \tilde{\mu} \quad (2.19)$$

Incorporation of Equations (2.18) and (2.19) into the equations of motion with the assumptions of constant velocity, small geometrical angles ($\bar{\gamma} = 1$), and the omission of gravity terms⁸ yields a second-order differential equation in the complex angle of attack

$$\tilde{\xi}'' + (H - iP)\tilde{\xi}' - (M + iPT)\tilde{\xi} = (R + iPS_{\gamma})\delta^2 e^{-i4\gamma} \tilde{\xi} + 3C_{N_{\gamma\delta^2}}^* \delta^2 e^{-i4\gamma} (\tilde{\xi})' \tilde{\xi} / \tilde{\xi} \quad (2.20)$$

where

$$H = C_{N_{\alpha_0}} - (C_{m_q}^* + C_{m_{\dot{\alpha}}}^*)k_t^{-2} \quad (2.21)$$

$$M = k_t^{-2}C_{m_{\alpha_0}}^* \quad (2.22)$$

$$T = C_{N_{\alpha_0}}^* + k_a^{-2}C_{m_{p\alpha}}^* \quad (2.23)$$

$$R = -k_t^{-2}C_{m_{\gamma\delta^2}}^* \quad (2.24)$$

and

$$S_{\gamma} = C_{N_{\gamma\delta^2}}^* \left[\frac{4I_y}{I_x} - 1 \right] \quad (2.25)$$

The axial and transverse radii of gyration are denoted by k_a and k_t respectively, and $(\bar{})$ denotes the complex conjugate. Note that the right-hand side of Equation (2.20) is composed of both lift and moment terms which are nonlinear in angle of attack. These nonlinearities are partially a result of the complex exponential $e^{-i4\gamma}$, as well as the nonlinear angle of attack dependence, as expressed in the Maple-Synge expansion.

C. DYNAMICS AND AERODYNAMICS OF ROLLING MOTION

The equation of rolling motion of a symmetric missile is also taken from Reference 8 and may be written simply as

$$I_x \dot{p} = q_{\infty} A d C_{\ell} \quad (2.26)$$

where C_{ℓ} is the total aerodynamic roll moment coefficient, which, for the purpose of the present analysis, is taken as the sum of a linear damping and a static aerodynamic roll moment, C_{ℓ_S} .

$$C_{\ell} = C_{\ell_P} \frac{pd}{V} + C_{\ell_S} \quad (2.27)$$

Now if the Maple-Synge symmetry arguments are applied in the case of the roll aerodynamics of a cruciform missile, it may be shown that the static roll moment terms must take the form (see the appendix)

$$C_{\ell_S} = \sum_{\ell=0}^{\infty} C_{0\ell} \delta^{2\ell} + \sum_{N=1}^{\infty} \delta^{4N} \sum_{\ell=0}^{\infty} \delta^{2\ell} B_{N\ell} \sin 4N\gamma \quad (2.28)$$

While this particular expansion is based on tetragonal symmetry, it does not require missile reflectional symmetry and hence can be used to account for fin misalignment.

Now if Equation (2.28) is expanded for the lowest-order terms ($\ell = 0$) and terms quintic in angle of attack and higher are omitted, it may be incorporated into Equation (2.26) to yield the differential equation of rolling motion to be considered

$$I_x \dot{p} = q_\infty A d \left\{ C_{\ell_0} + C_{\ell_p} \frac{pd}{V} + C_{\ell_{\gamma \delta^4}} \delta^4 \sin 4\gamma + \dots \right\} \quad (2.29)$$

where the coefficients in the formal Maple-Syngé expansion have been replaced with the more familiar C_{ℓ_0} (roll driving), and $C_{\ell_{\gamma \delta^4}}$ (induced roll). It should be noted that while Equation (2.29) contains the lowest-order terms which describe the induced roll moment, the δ^2 , δ^4 dependence of the roll driving moment coefficient has been omitted, since these terms display no roll orientation dependence. Hence their retention was not considered essential in the present study of induced rolling motion.

Typical induced rolling moment coefficient behavior with roll angle is shown plotted in Figure 5 together with yaw moment coefficient data taken on a cruciform missile configuration at subsonic Mach numbers. Also shown plotted are the analytical approximations to the data which resulted from a least-squares fit with the Maple-Syngé functional form.

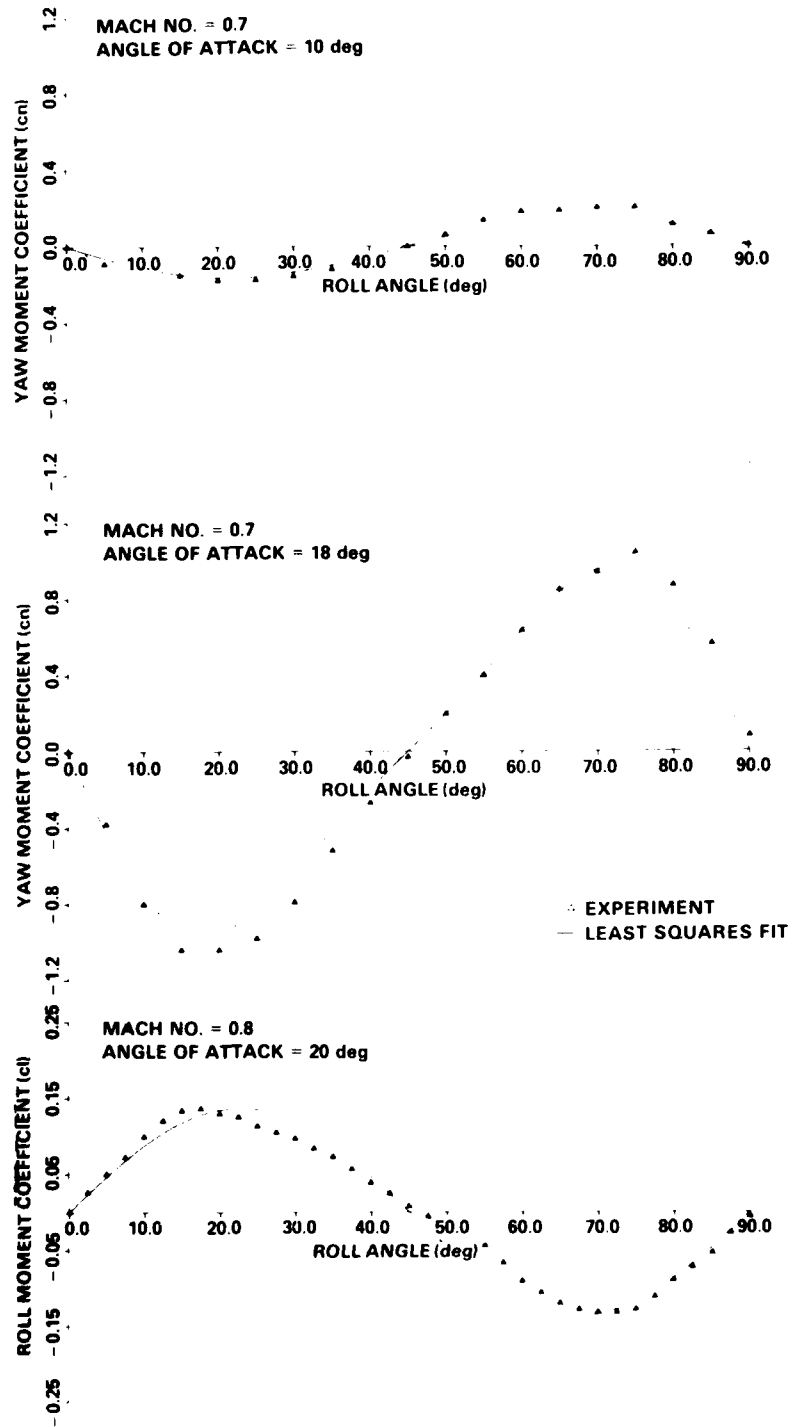


Figure 5. - Typical Induced Rolling Moment Coefficient Behavior (Reference 11)

CHAPTER III

ANGULAR MOTION WITH PRESCRIBED ROLLING MOTION

A. NONRESONANT SOLUTIONS

The full nonlinear problem of pitch, yaw, and rolling motion, in the presence of roll orientation-dependent aerodynamics is the ultimate objective of this analysis. However, it will be instructive in what follows to partially decouple the motion by considering the transverse angular motion with the rolling motion prescribed a priori. While this is not representative of the free-flight condition, it hopefully will exhibit the effects of the roll-dependent forces and moments on missile stability and provide insight that will be useful in the solution of the full coupled problem.

In this chapter a solution is sought to the differential equations of yawing motion, in the presence of roll orientation-dependent aerodynamics, where the roll rate is, at most, slowly varying in comparison with the frequency of the yawing motion.

An inspection of the nonlinear roll-dependent terms on the right-hand side of Equation (2.20) reveals that the imaginary part of the coefficient $R + iPS_\gamma$ is quite small in comparison with R for roll rates characteristic of a finned missile, and hence may be approximated by the real part only. In like manner, it can be shown* that the lift term containing $C_{N_\gamma\delta^2}$ is several orders of magnitude smaller than the moment term and will therefore be neglected.

In the development of the approximate solutions which follow it will be instructive and more physically meaningful to change the independent variable of Equation (2.20) from arclength to time which is easily accomplished through the use of Equation (2.9) and the assumption of constant velocity. With the above approximations in mind, Equation (2.20) may be rearranged and written in the time domain as

$$\ddot{\xi} - iP_0\dot{\xi} - \omega_0^2\xi = \epsilon^2\mu_1\dot{\xi} + i\epsilon^2\mu_2\ddot{\xi} + \chi_1\delta^2e^{-i4\gamma}\ddot{\xi}$$

where

$$\begin{aligned} P_0 &= pI_x/I_y \\ \omega_0^2 &= MV^2/d^2 \\ \epsilon^2\mu_1 &= -HV/d \\ \epsilon^2\mu_2 &= P_0TV/d \\ \chi_1 &= RV^2/d^2 \\ \delta^2 &= \ddot{\xi}\ddot{\xi} \end{aligned} \tag{3.1}$$

*The term $\ddot{\xi}/\dot{\xi}$ is proportional to the frequency of the yawing motion which for normal epicyclic motion is usually on the order of 10^{-3} rad/cal.

and ϵ is a small dimensionless quantity of order δ which has been introduced into the linear damping and Magnus terms such that the forcing terms to the unperturbed differential equation are of order δ^3 .

In order to obtain an approximate solution to Equation (25) with roll-dependent aerodynamics and constant spin via the method of multiple scales, two independent time scales T_0 and T_2 are introduced such that

$$t = T_0 + \epsilon^2 T_2 \quad (3.2)$$

Here the fast time scale T_0 is associated with the yawing motion, while the slow time scale T_2 is associated with quantities changing slowly along the trajectory such as dynamic pressure, aerodynamic coefficients, etc. Thus, derivatives with respect to time t , are transformed to partial derivatives according to

$$\frac{d}{dt} = \frac{\partial}{\partial T_0} + \epsilon^2 \frac{\partial}{\partial T_2} \quad (3.3)$$

A solution to Equation (3.1) is sought in the form of an asymptotic expansion in the smallness parameter ϵ of the form:

$$\tilde{\xi}(t) = \epsilon \tilde{\xi}_1(T_0, T_2) + \epsilon^3 \tilde{\xi}_3(T_0, T_2) + \dots \quad (3.4)$$

which remains uniformly valid. This is equivalent to the condition that $\tilde{\xi}_3/\tilde{\xi}_1$ remains bounded for all T_0 and T_2 . The introduction of the smallness parameter ϵ , into the equations of motion and the assumed form of the asymptotic expansion for $\tilde{\xi}(t)$ may, at first, seem somewhat arbitrary. However, a successful application of the method of multiple scales transforms the nonlinear differential Equation (3.1) to a sequence of linear partial differential equations in the $\tilde{\xi}_j(t)$.

Substituting Equation (3.4) into Equation (3.1) while making use of Equation (3.3) and equating equal powers of ϵ one obtains

$$\frac{\partial^2 \tilde{\xi}_1}{\partial T_0^2} - iP_0 \frac{\partial \tilde{\xi}_1}{\partial T_0} - \omega_0^2 \tilde{\xi}_1 = 0 \quad (3.5)$$

$$\frac{\partial^2 \tilde{\xi}_3}{\partial T_0^2} - iP_0 \frac{\partial \tilde{\xi}_3}{\partial T_0} - \omega_0^2 \tilde{\xi}_3 = \frac{-2\partial^2 \tilde{\xi}_1}{\partial T_0 \partial T_2} + iP_0 \frac{\partial \tilde{\xi}_1}{\partial T_2} + \mu_1 \frac{\partial \tilde{\xi}_1}{\partial T_0} + i\mu_2 \tilde{\xi}_1 + \chi_1 (\tilde{\xi}_1)^3 e^{i4\phi} \quad (3.6)$$

The general solution to Equation (3.5) is the usual epicyclic solution

$$\tilde{\xi}_1(T_0, T_2) = K_1(T_2)e^{i\omega_1 T_0} + K_2(T_2)e^{i\omega_2 T_0} \quad (3.7)$$

where ω_1 and ω_2 are the nutation and precession frequencies respectively, given by

$$\omega_{1,2} = \frac{1}{2} \left(P_0 \pm \sqrt{P_0^2 - 4\omega_0^2} \right) \quad (3.8)$$

Having obtained a solution to Equation (3.5), Equation (3.7) may be substituted into Equation (3.6) to obtain

$$\begin{aligned} \frac{\partial^2 \tilde{\xi}_3}{\partial T_0^2} - iP_0 \frac{\partial \tilde{\xi}_3}{\partial T_0} - \omega_0^2 \tilde{\xi}_3 = w_1 e^{i\omega_1 T_0} + w_2 e^{i\omega_2 T_0} \\ + \chi_1 e^{i4\phi_0} \left\{ \bar{K}_1^3 e^{i(4p-3\omega_1)T_0} + 2\bar{K}_1^2 \bar{K}_2 e^{i(4p-2\omega_1-\omega_2)T_0} \right. \\ + \bar{K}_2^2 \bar{K}_1 e^{i(4p-2\omega_2-\omega_1)T_0} + \bar{K}_1^2 \bar{K}_2 e^{i(4p-2\omega_1-\omega_2)T_0} \\ \left. + 2\bar{K}_1 \bar{K}_2^2 e^{i(4p-\omega_1-2\omega_2)T_0} + \bar{K}_2^3 e^{i(4p-3\omega_2)T_0} \right\} \end{aligned} \quad (3.9)$$

where

$$w_1 = i(P_0 - 2\omega_1) \frac{dK_1}{dT_2} + i\mu_1 K_1 \omega_1 + i\mu_2 K_1 \quad (3.10)$$

and

$$w_2 = i(P_0 - 2\omega_2) \frac{dK_2}{dT_2} + i\mu_1 K_2 \omega_2 + i\mu_2 K_2 \quad (3.11)$$

Implicit in Equation (3.9) is the assumption of constant spin such that

$$\phi = \phi_0 + pT_0 \quad (3.12)$$

Now particular solutions to Equation (3.9) contain secular terms of the form $T_0 e^{i\omega_j T_0}$, which, as T_0 becomes large, cause $\tilde{\xi}_3/\xi_1$ to become unbounded. Therefore, to obtain a uniformly valid expansion, the K_j are chosen such that the secular terms vanish, i.e., $w_j = 0$. The complex modal vectors, K_j may be represented by their respective amplitude and phase and substituted into Equations (3.10) and (3.11) while separating real and imaginary parts to obtain the modal damping and phase differential equations:

$$\frac{dk_1}{dT_2} = -\frac{(\mu_1 \omega_1 + \mu_2)}{P_0 - 2\omega_1} \quad (3.13)$$

$$\frac{dk_2}{dT_2} = -\frac{(\mu_1 \omega_2 + \mu_2)}{P_0 - 2\omega_2} \quad (3.14)$$

$$\frac{d\theta_1}{dT_2} = \frac{d\theta_2}{dT_2} = 0 \quad (3.15)$$

where

$$K_j = k_j e^{i\theta_j} \quad (3.16)$$

With the secular terms removed, Equation (3.9) may now be solved for $\tilde{\xi}_3$ to obtain

$$\tilde{\xi}_3(T_0, T_2) = -\chi_1 \left\{ \frac{\bar{K}_1^3 e^{i\nu_1 T_0}}{\nu_1^2 - P_0 \nu_1 + \omega_0^2} + \frac{\bar{K}_2^3 e^{i\nu_2 T_0}}{\nu_2^2 - P_0 \nu_2 + \omega_0^2} + \frac{3\bar{K}_1^2 \bar{K}_2 e^{i\nu_3 T_0}}{\nu_3^2 - P_0 \nu_3 + \omega_0^2} + \frac{3\bar{K}_1 \bar{K}_2^2 e^{i\nu_4 T_0}}{\nu_4^2 - P_0 \nu_4 + \omega_0^2} \right\} \quad (3.17)$$

where

$$\begin{aligned} \nu_1 &= 4p - 3\omega_1 \\ \nu_2 &= 4p - 3\omega_2 \\ \nu_3 &= 4p - 2\omega_1 - \omega_2 \\ \nu_4 &= 4p - \omega_1 - 2\omega_2 \end{aligned} \quad (3.18)$$

Thus the complete solution $\tilde{\xi}(T_0, T_2)$ up to order ϵ^3 may be written

$$\begin{aligned} \tilde{\xi}(T_0, T_2) &= \epsilon K_1 e^{i\omega_1 T_0} + \epsilon K_2 e^{i\omega_2 T_0} - \epsilon^3 \chi_1 \left\{ \frac{\bar{K}_1^3 e^{i\nu_1 T_0}}{\nu_1^2 - P_0 \nu_1 + \omega_0^2} \right. \\ &\quad \left. + \frac{\bar{K}_2^3 e^{i\nu_2 T_0}}{\nu_2^2 - P_0 \nu_2 + \omega_0^2} + \frac{3\bar{K}_1^2 \bar{K}_2 e^{i\nu_3 T_0}}{\nu_3^2 - P_0 \nu_3 + \omega_0^2} + \frac{3\bar{K}_1 \bar{K}_2^2 e^{i\nu_4 T_0}}{\nu_4^2 - P_0 \nu_4 + \omega_0^2} \right\} \end{aligned} \quad (3.19)$$

Equations (3.13) through (3.15) indicate that to a first approximation, for nonresonant motion, the behavior of the modal amplitudes is unaffected by the presence of the roll-orientation-dependent aerodynamics.* Figure 6 shows a comparison between solutions generated with Equation (3.19) and a direct numerical solution of Equation (3.1).

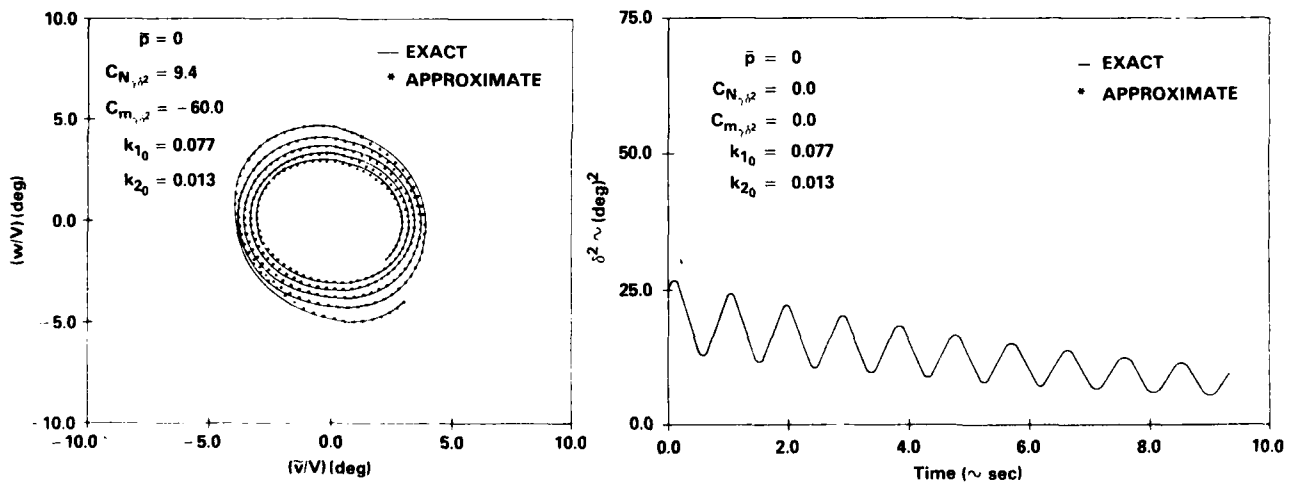


Figure 6. - Comparison of Approximate and Exact Solutions: Nonresonant Spin

*Identical results may also be generated, using the method of averaging. (Reference 15)

Missile aerodynamic and inertial characteristics used in the calculations may be found in Table 1.

It should be noted that Equation (3.19) becomes singular when $\nu_j = \omega_{1,2}$. A close inspection of possible singular roll rates reveals that Equation (3.19) ceases to be valid at zero spin, $p = \omega_1$ and approximately one-half resonant spin $p \approx (3\omega_1 + \omega_2)/4$. At these roll rates, ν_j approaches either ω_1 or ω_2 , which introduces additional secular terms into Equation (3.9) which were previously not taken into account.

B. RESONANT SPIN

Solutions which are valid at resonant spin may be generated by a consideration of Equation (3.9) with $\nu_1 = \omega_1$ to obtain:

$$\begin{aligned} \frac{\partial^2 \tilde{\xi}_3}{\partial T_0^2} - iP_0 \frac{\partial \tilde{\xi}_3}{\partial T_0} - \omega_0^2 \tilde{\xi}_3 = & [w_1 + \chi_1 \bar{K}_1^3 e^{i4\phi_0}] e^{i\omega_1 T_0} \\ & + w_2 e^{i\omega_2 T_0} + \chi_1 e^{i4\phi_0} [\bar{K}_2^3 e^{i(4\omega_1 - 3\omega_2)T_0} \\ & + 3\bar{K}_1^2 \bar{K}_2 e^{i(2\omega_1 - \omega_2)T_0} + 3\bar{K}_1 \bar{K}_2^2 e^{i(3\omega_1 - 2\omega_2)T_0}] \end{aligned} \quad (3.20)$$

With the elimination of secular terms, the damping and phase differential equations for the variation of the modal amplitudes take the form

$$i(P_0 - 2\omega_1) \frac{dK_1}{dT_2} + i\mu_1 K_1 \omega_1 + i\mu_2 K_1 + \chi_1 e^{i4\phi_0} \bar{K}_1^3 = 0 \quad (3.21)$$

$$i(P_0 - 2\omega_2) \frac{dK_2}{dT_2} + i\mu_1 K_2 \omega_2 + i\mu_2 K_2 = 0 \quad (3.22)$$

With secular terms eliminated, Equation (3.20) may now be solved for $\tilde{\xi}_3(T_0, T_2)$ which is valid only at resonance ($p = \omega_1$) to yield

$$\tilde{\xi}_3(T_0, T_2) = \chi_1 e^{i4\phi_0} \left[\frac{\bar{K}_2^3 e^{in_1 T_0}}{n_1^2 - P_0 n_1 + \omega_0^2} + \frac{3\bar{K}_1^2 \bar{K}_2 e^{in_2 T_0}}{n_2^2 - P_0 n_2 + \omega_0^2} + \frac{3\bar{K}_1 \bar{K}_2^2 e^{in_3 T_0}}{n_3^2 - P_0 n_3 + \omega_0^2} \right] \quad (3.23)$$

where

$$\begin{aligned} n_1 &= 4\omega_1 - 3\omega_2 \\ n_2 &= 2\omega_1 - \omega_2 \\ n_3 &= 3\omega_1 - 2\omega_2 \end{aligned} \quad (3.24)$$

The complete solution $\tilde{\xi}(T_0, T_2)$, valid at resonant spin, may now be written

$$\begin{aligned} \tilde{\xi}(T_0, T_2) = \epsilon K_1 e^{i\omega_1 T_0} + \epsilon K_2 e^{i\omega_2 T_0} + \epsilon^3 \chi_1 e^{i4\phi_0} & \left[\frac{\bar{K}_2^3 e^{in_1 T_0}}{n_1^2 - P_0 n_1 + \omega_0^2} \right. \\ & \left. + \frac{3\bar{K}_1^2 \bar{K}_2 e^{in_2 T_0}}{n_2^2 - P_0 n_2 + \omega_0^2} + \frac{3\bar{K}_1 \bar{K}_2^2 e^{in_3 T_0}}{n_3^2 - P_0 n_3 + \omega_0^2} \right] \end{aligned} \quad (3.25)$$

Table 1. – Missile Aerodynamics and Configurational Characteristics

MACH NUMBER	0.78
FLIGHT ALTITUDE	6000 km
REFERENCE DIAMETER, d	27.3 cm
MASS, m	272.1 kgm
POLAR MOMENT OF INERTIA	2.7 kgm – m ²
TRANSVERSE MOMENT OF INERTIA	54.5 kgm – m ²

AERODYNAMICS

$C_{N_\alpha} = 4.30$	$C_{mq} + C_{M_{\dot{\alpha}}} = -50.0$
$C_{m_\alpha} = -4.20$	$C_{m_{p_\alpha}} = 5.00$
$C_{N_{\gamma\delta^2}} = 9.1$	$C_{\ell_0} = 0.20$
$C_{m_{\gamma\delta^2}} = -30.8$	$C_{\ell_{\gamma\delta^4}} = 10.6$
	$C_{\ell_p} = -2.0$

Several important comments regarding the distinction between Equations (3.19) and (3.25) should be made. While Equation (3.19) is valid for all spin except $p = 0, \omega_1/2, \omega_1$, Equation (3.25) is valid at $p = \omega_1$ only. For non-resonant spin, the effect of the roll-dependent aerodynamics was not discernible. However, at resonance ($p = \omega_1$), the nutation amplitude may be strongly affected by χ_1 and ϕ_0 . This characteristic of sensitivity of the stability of the motion to initial conditions gives some insight into the mechanism of resonance-related instabilities whereby the missile stability is dependent upon the amplitude as well as the initial phase of the motion.

The validity of Equation (3.25) was checked by comparison with direct solutions of Equation (3.1) at resonant spin and the results of these calculations are shown in Figures 7 through 10 where two identical configurations are released at slightly different initial conditions. Figure 8 is seen to depict stable motion while the motion of Figure 10 shows the configuration to be slightly unstable.

Additional insight into the sensitivity of the motion at resonant spin to variations in initial conditions may be gained through a decomposition of Equation (3.21) and displaying the slowly varying dynamics of the two-dimensional system in an amplitude-phase plane. Separating Equation (3.21) into real and imaginary parts, the nutation mode behavior may be represented by

$$\frac{dk_1}{dT_2} = -\left(\frac{\mu_1 \omega_1 + \mu_2}{P_0 - 2\omega_1}\right) k_1 - \frac{\chi_1}{P_0 - 2\omega_1} k_1^3 \sin \beta_0 \quad (3.26)$$

$$\frac{d\theta_1}{dT_2} = \frac{\chi_1}{P_0 - 2\omega_1} k_1^2 \cos \beta_0 \quad (3.27)$$

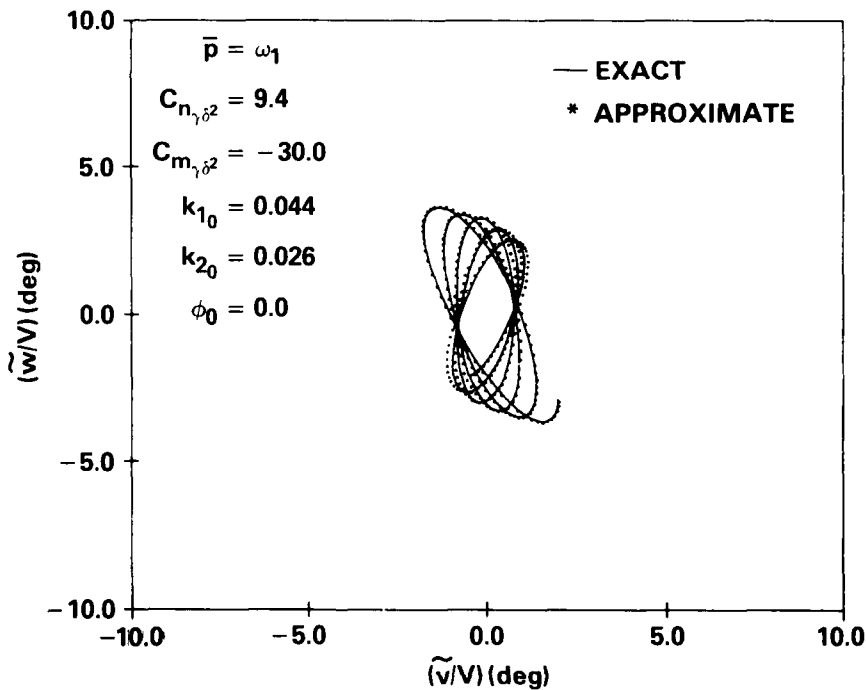


Figure 7. - Complex Angle of Attack History at Fundamental Resonance with Nonlinear, Roll-Dependent Aerodynamics

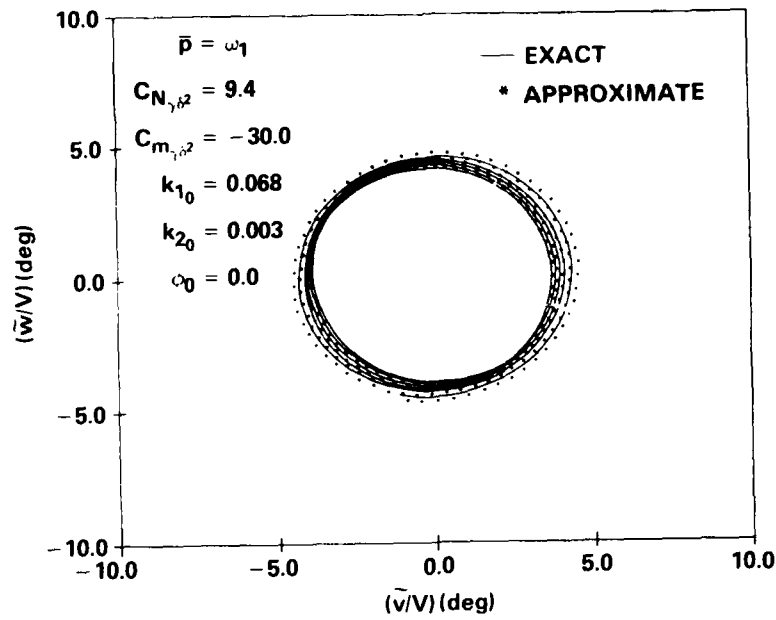


Figure 8. - Missile Transient Response at Fundamental Resonance with Nonlinear, Roll-Dependent Aerodynamics

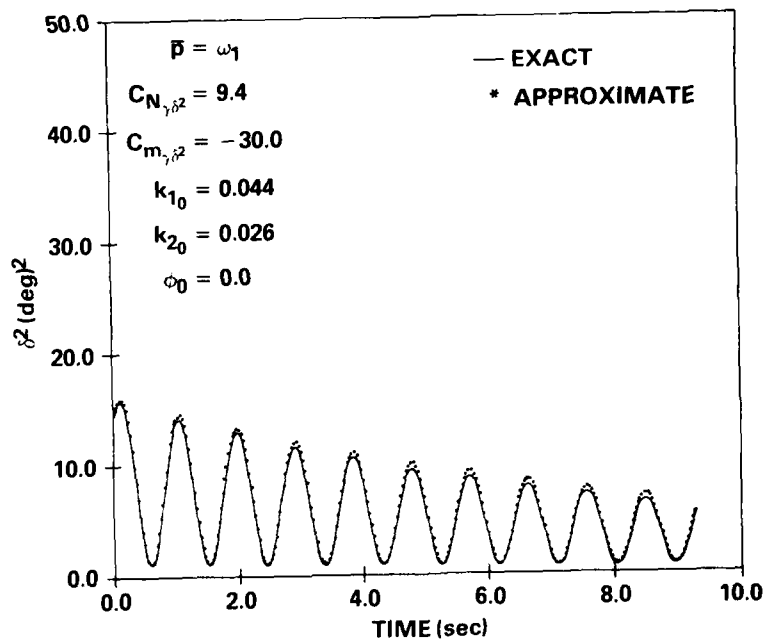


Figure 9. - Complex Angle of Attack History at Fundamental Resonance with Nonlinear, Roll-Dependent Aerodynamics

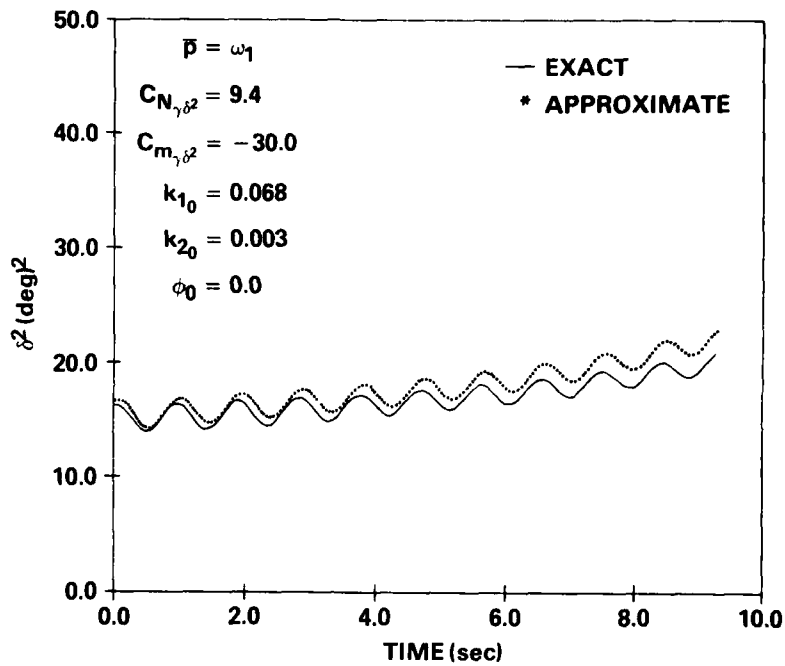


Figure 10. - Missile Transient Response at Fundamental Resonance with Nonlinear, Roll-Dependent Aerodynamics

where

$$\beta_0 = 4(\phi_0 - \theta_1) \quad (3.28)$$

Solutions to Equations (3.26) and (3.27) are shown as trajectories in the $k_1^2 - \beta_0$ plane of Figure 11. Initial conditions leading to stable motion are seen to be those originating below the dashed line denoted as the separatrix. It is now clear that the principal features determining the stability of the missile at resonance are the amplitude of the nutation component k_1 , and the relative phase, β_0 .

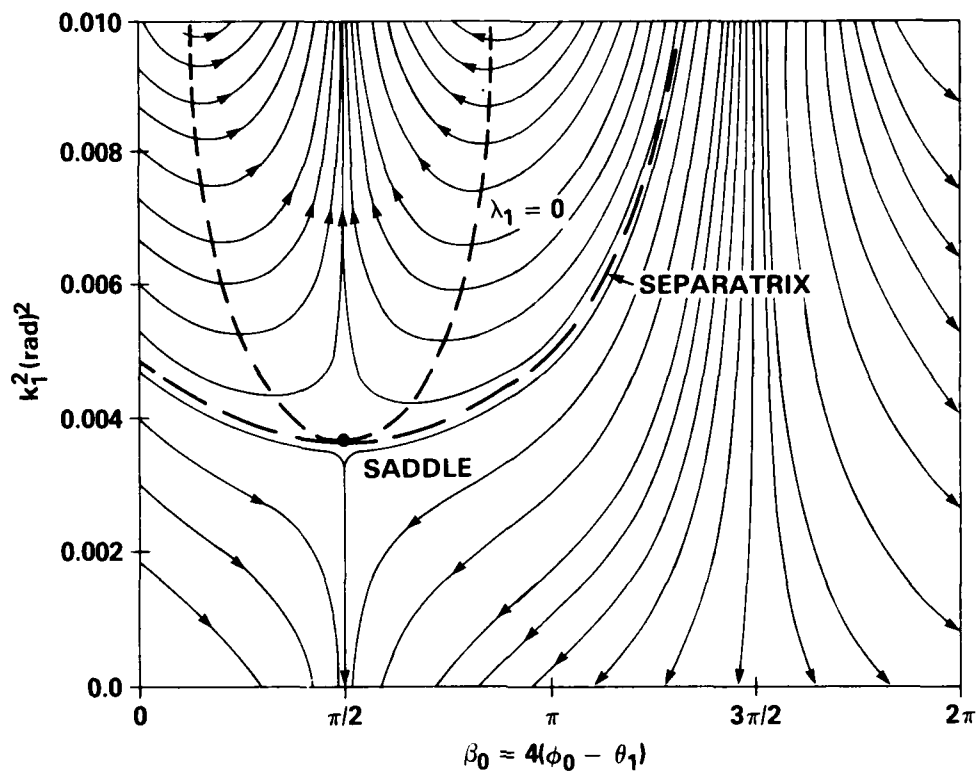


Figure 11. - Phase Plane at Fundamental Resonance ($p = \omega_1$)

CHAPTER IV

INDUCED ROLLING MOTION WITH PRESCRIBED YAWING MOTION

In the previous chapter, attention was focused on the nonlinear yawing motion, while the rolling motion was constrained at constant roll rate. While this can hardly be considered representative of free-flight conditions, considerable insight was gained into the effect of the roll-dependent side moment on missile stability. In this chapter, this philosophy is applied in a study of the induced rolling motion where a solution to the nonlinear roll dynamics is sought while the yawing motion is constrained to be epicyclic.

A. NONRESONANT SOLUTIONS

The roll differential equation, Equation (2.29), which was previously derived in Chapter II to include the lowest-order roll-dependent terms consistent with the Maple-Syngé expansion, may be rewritten in slightly different form with the introduction of the smallness parameter ϵ , whose magnitude is of the order of the total angle of attack, as

$$\frac{dp}{dt} = \epsilon^2 \left\{ \sigma_0 + \sigma_2 p + \sigma_1 \operatorname{Im}(\tilde{\xi}^4 e^{-i4\phi}) \right\}$$

where

$$\epsilon^2 \sigma_0 = \frac{q_\infty A d}{I_x} C_{\ell_0} \quad (4.1)$$

$$\epsilon^2 \sigma_1 = \frac{q_\infty A d}{I_x} C_{\ell_{\gamma\delta^4}}$$

$$\epsilon^2 \sigma_2 = \frac{q_\infty A d^2}{V I_x} C_{\ell_p}$$

Approximate solutions to Equation (4.1) are sought using the generalized version of the method of multiple scales.⁵ If Equation (4.1) is considered in the absence of the induced roll term, the solution exhibits the usual slowly varying, exponential behavior of the roll rate, which is associated with the slow time scale T_2 such that

$$\frac{d}{dt} = \epsilon^2 \frac{\partial}{\partial T_2} \quad (4.2)$$

Inclusion of the induced roll term introduces a nonlinear forcing function whose excitation will be dependent upon the amplitude and frequency of the assumed missile angular motion, $\xi(t)$. If the familiar epicyclic motion of a symmetric missile is assumed, it is evident that the resulting solution $p(t)$ should contain components whose frequencies are linear combinations of the epicyclic frequencies ω_1 and ω_2 . In view of this, it is assumed that $\tilde{\xi}(t)$ is given by

$$\tilde{\xi}(t) = \sum_{j=1}^2 K_j e^{i\psi_j} \quad (4.3)$$

where

$$\frac{d\psi_j}{dt} = \omega_j \quad (4.4)$$

and the asymptotic expansion for $p(t; \epsilon)$ is of the form

$$p(t; \epsilon) = p_0(T_2) + \epsilon^2 p_2(\psi_1, \psi_2, \phi, T_2) + \dots \quad (4.5)$$

Thus time derivatives of $p(t)$ will be converted to partial derivatives with the independent variables ψ_j , ϕ , and T_2 .

Substitution of Equation (4.5) into Equation (4.1) while making use of Equations (4.2) and (4.4), and equating all terms of order ϵ^2 results in the linear partial differential equation

$$\begin{aligned} \omega_1 \frac{\partial p_2}{\partial \psi_1} + \omega_2 \frac{\partial p_2}{\partial \psi_2} + p_0 \frac{\partial p_2}{\partial \phi} = & w_3(T_2) + \sigma_1 \text{Im} [K_1^4 e^{i4(\psi_1 - \phi)} \\ & + K_2^4 e^{i4(\psi_2 - \phi)} + 4K_1^3 K_2 e^{i(3\psi_1 + \psi_2 - 4\phi)} \\ & + 6K_1^2 K_2^2 e^{2i(\psi_1 + \psi_2 - 2\phi)} \\ & + 4K_1 K_2^3 e^{i(\psi_1 + 3\psi_2 - 4\phi)}] \end{aligned} \quad (4.6)$$

where

$$w_3(T_2) = -\frac{dp_0}{dT_2} + \sigma_2 p_0 + \sigma_0 \quad (4.7)$$

and

$$K_j = k_j e^{i\theta_j} \quad (4.8)$$

Particular solutions to Equation (4.6) become unbounded as ψ_j and ϕ become large. Therefore, it is required that the secular term w_3 vanish, yielding the differential equation

$$\frac{dp_0}{dT_2} = \sigma_0 + \sigma_2 p_0 \quad (4.9)$$

for the slowly varying spin. With the exclusion of the secular term, a particular solution to Equation (4.6) may be found

$$\begin{aligned}
p_2(t) = & \frac{\sigma_1 k_1^4}{4(p_0 - \omega_1)} \cos 4(\hat{\psi}_1 - \phi) + \frac{\sigma_1 k_2^4}{4(p_0 - \omega_2)} \cos 4(\hat{\psi}_2 - \phi) \\
& + \frac{4\sigma_1 k_1^3 k_2}{4p_0 - 3\omega_1 - \omega_2} \cos(3\hat{\psi}_1 + \hat{\psi}_2 - 4\phi) + \frac{3\sigma_1 k_1^2 k_2^2}{2p_0 - \omega_1 - \omega_2} \cos 2(\hat{\psi}_1 + \hat{\psi}_2 - 2\phi) \\
& + \frac{4\sigma_1 k_1 k_2^3}{4p_0 - \omega_1 - 3\omega_2} \cos(\hat{\psi}_1 + 3\hat{\psi}_2 - 4\phi)
\end{aligned} \tag{4.10}$$

Solving Equation (4.7) for $p_0(T_2)$, the complete expansion for $p(t)$, with induced rolling moment in the presence of epicyclic yawing motion becomes

$$\begin{aligned}
p(t; \epsilon) = & p_0(0)e^{\sigma_2 T_2} + \frac{\sigma_0}{\sigma_2} (e^{\sigma_2 T_2} - 1) + \epsilon^2 \sigma_1 \left[\frac{k_1^4}{4(p_0 - \omega_1)} \cos 4(\hat{\psi}_1 - \phi) \right. \\
& + \frac{k_2^4}{4(p_0 - \omega_2)} \cos 4(\hat{\psi}_2 - \phi) + \frac{4k_1^3 k_2}{4p_0 - 3\omega_1 - \omega_2} \cos(3\hat{\psi}_1 + \hat{\psi}_2 - 4\phi) \\
& \left. + \frac{3k_1^2 k_2^2}{2p_0 - \omega_1 - \omega_2} \cos 2(\hat{\psi}_1 + \hat{\psi}_2 - 2\phi) + \frac{4k_1 k_2^3}{4p_0 - \omega_1 - 3\omega_2} \cos(\hat{\psi}_1 + 3\hat{\psi}_2 - 4\phi) \right]
\end{aligned} \tag{4.11}$$

Inspection of Equation (4.11) again reveals the existence of discrete, singular roll rates at which the solution is no longer valid. If the denominators of the ϵ^2 -terms of Equation (4.11) are allowed to vanish, considering only positive values of p_0 , the three singular roll rates are identified as

$$\begin{aligned}
p_0 &= \omega_1 \\
p_0 &= (3\omega_1 + \omega_2)/4 \\
p_0 &= (\omega_1 + \omega_2)/2
\end{aligned} \tag{4.12}$$

which are identical to the singular roll rates resulting from the case of constrained rolling motion of Chapter III. Since the functional forms of the induced yawing moment, and induced roll moment are quite similar, this result is not surprising.

B. RESONANT SOLUTIONS

When the rolling velocity is in the vicinity of the above singular roll rates, additional resonant solutions must be generated which are valid in the vicinity of these points. If Equation (4.6) is considered in the vicinity of fundamental resonance, and if the ψ_j are interpreted as $\omega_j T_0$, it is evident that the term $\sigma_1 K_1^4 \exp[4i(\psi_1 - \phi)]$ will be stationary for perfect resonance, $p = \omega_1$. For roll rates in the vicinity of resonance, $p_0 \approx \omega_1$, this term will, at most, be a slowly varying function of time, T_2 , and hence will give rise to secular terms in the expansion $p(t)$. Therefore, in order that the solution remain valid for large time, it is required that

$$-\frac{dp_0}{dT_2} + \sigma_2 p_0 + \sigma_0 + \sigma_1 k_1^4 \sin 4(\hat{\psi}_1 - \phi) = 0 \tag{4.13}$$

Equation (4.6) then becomes

$$\begin{aligned} \omega_1 \frac{\partial p_2}{\partial \psi_1} + \omega_2 \frac{\partial p_2}{\partial \psi_2} + p_0 \frac{\partial p_2}{\partial \phi} = \sigma_1 \text{Im} \left[K_2^4 e^{i4(\psi_2 - \phi)} + 4K_1^3 K_2 e^{i(3\psi_1 + \psi_2 - 4\phi)} \right. \\ \left. + 6K_1^2 K_2^2 e^{2i(\psi_1 - \psi_2 - 2\phi)} + 4K_1 K_2^3 e^{i(\psi_1 + 3\psi_2 - 4\phi)} \right] \end{aligned} \quad (4.14)$$

which displays a particular solution valid at $p_0 = \omega_1$:

$$\begin{aligned} p_2(t) = \frac{\sigma_1 k_2^4}{4(p_0 - \omega_2)} \text{Cos } 4(\hat{\psi}_2 - \phi) + \frac{4\sigma_1 k_1^3 k_2}{4p_0 - 3\omega_1 - \omega_2} \text{Cos } (3\hat{\psi}_1 + \hat{\psi}_2 - 4\phi) \\ + \frac{3\sigma_1 k_1^2 k_2^2}{2p_0 - \omega_1 - \omega_2} \text{Cos } 2(\psi_1 + \psi_2 - 2\phi) + \frac{4\sigma_1 k_1 k_2^3}{4p_0 - \omega_1 - 3\omega_2} \text{Cos } (\psi_1 + 3\psi_2 - 4\phi) \end{aligned} \quad (4.15)$$

In like manner, approximate solutions which are valid at zero spin, $p_0 = \omega_1 + \omega_2$, and one-half resonant spin, $p_0 = (3\omega_1 + \omega_2)/4$ may also be generated. For zero spin, the variation of the first-order solution $p_0(t)$ is given by

$$\frac{dp_0}{dT_2} = \sigma_2 p_0 + \sigma_0 + \sigma_1 k_1^2 k_2^2 \text{Sin } 2(\hat{\psi}_1 + \hat{\psi}_2 - 2\phi) \quad (4.16)$$

while the second-order term in the expansion is found to be

$$\begin{aligned} p_2(t) = \frac{\sigma_1 k_1^4}{4(p_0 - \omega_1)} \text{Cos } 4(\hat{\psi}_1 - \phi) + \frac{\sigma_1 k_2^4}{4(p_0 - \omega_2)} \text{Cos } 4(\hat{\psi}_2 - \phi) \\ + \frac{4\sigma_1 k_1^3 k_2}{4p_0 - 3\omega_1 - \omega_2} \text{Cos } (3\hat{\psi}_1 + \hat{\psi}_2 - 4\phi) + \frac{4\sigma_1 k_1 k_2^3}{4p_0 - \omega_1 - 3\omega_2} \text{Cos } (\hat{\psi}_1 + 3\hat{\psi}_2 - 4\phi) \end{aligned} \quad (4.17)$$

Finally, the first-order rolling motion at one-half resonant spin is governed by

$$\frac{dp_0}{dT_2} = \sigma_2 p_0 + \sigma_0 + 4\sigma_1 k_1^3 k_2 \text{Sin } (3\hat{\psi}_1 + \hat{\psi}_2 - 4\phi) \quad (4.18)$$

and the second-order solution becomes

$$\begin{aligned} p_2(t) = \frac{\sigma_1 k_1^4}{4(p_0 - \omega_1)} \text{Cos } 4(\hat{\psi}_1 - \phi) + \frac{\sigma_1 k_2^4}{4(p_0 - \omega_2)} \text{Cos } 4(\hat{\psi}_2 - \phi) \\ + \frac{3k_1^2 k_2^2}{2p_0 - \omega_1 - \omega_2} \text{Cos } 2(\hat{\psi}_1 + \hat{\psi}_2 - 2\phi) + \frac{4k_1 k_2^3}{4p_0 - \omega_1 - 3\omega_2} \text{Cos } (\hat{\psi}_1 + 3\hat{\psi}_2 - 4\phi) \end{aligned} \quad (4.19)$$

It should be emphasized that Equations (4.13) through (4.19) are valid for the discrete roll rates only.

A direct comparison of the approximate solutions to Equation (4.1) using the method of multiple scales with direct numerical solutions is complicated by the singular nature of the problem at the three discrete roll rates mentioned above. Typical roll rates of interest for operational air-launched ordnance range from zero spin to the onset of Magnus instability which is usually several times resonance. Therefore a comparison of the approximate solutions of this chapter with direct numerical integrations of Equation (4.1), over spin rates of interest will necessitate the use of multiple resonant and nonresonant solutions which must be "matched" in an appropriate manner such that continuous coverage of the roll spectrum is achieved.

In practice, this matching is achieved through the introduction of a detuning parameter λ , which is used to slightly detune the singular solution as the roll rate varies about the singular roll rate. For example, in the case of fundamental resonance, the roll rate is detuned according to

$$p = \omega_1 + \lambda \epsilon^2 \quad (4.20)$$

where $\nu = 0(1)$. Substitution of Equation (4.20) into Equation (4.13) yields

$$\frac{dp_0}{dT_2} = \sigma_2 p_0 + \sigma_0 + \sigma_1 k_1^4 \sin 4(\theta_1 - \phi_0 - \lambda T_2) \quad (4.21)$$

Thus, through the introduction of the parameter λ , the "matched" asymptotic expansions of Equation (4.5) can be used to describe the nonlinear rolling motion over the entire spectrum of roll frequencies.

Figures 12 through 18 display the missile induced rolling motion for yawing motion of various amplitudes. Missile physical properties and aerodynamic characteristics used in the calculations were shown in Table 1. For the purposes of these calculations, approximate solutions generated by the method of multiple scales, were matched at points which were chosen to lie midway between resonant roll rates. While more elaborate methods may be devised, the present method proved reasonably successful as evidenced by the agreement displayed in Figures 12 through 18 for a variety of initial conditions and design roll rates. These results display the dependence of the roll rate history on initial conditions and angle of attack for a passage through resonance to the design roll rate of $3\omega_1$. As the amplitude of the yawing motion increases, the rolling motion becomes dominated by the large induced roll effects, and the validity of the perturbation analysis becomes questionable at angles of attack in the neighborhood of 30 degrees. In addition, the inaccuracy of the asymptotic expansion of Equation (4.5) for large time, is evidenced by the growing phase difference between the approximate and exact solutions.

Missile roll behavior in the vicinity of resonance may be demonstrated by an inspection of Equation (4.13) together with an analysis of the following numerical results. Figures 19 through 21 show missile roll rate histories passing from resonance ($p_0 = \omega_1$) to a design roll rate of $3\omega_1$, under the influence of progressively larger yawing motion which is predominantly precessional. As predicted by Equation (65), the roll rate approaches its design value with only minor variations even as the amplitude of the yawing motion approaches some 30 degrees.

Stability of the rolling motion at resonance is demonstrated by the results of Figures 22 through 27 where the missile design roll rate was chosen as $p_{ss} = \omega_1$. The diminished influence of large amplitude precessional motion is again displayed by the results of Figures 22 and 23 while Figures 25, 26, and 27 indicate the drastic change in the character of the rolling motion under the influence of large-amplitude nutational motion.

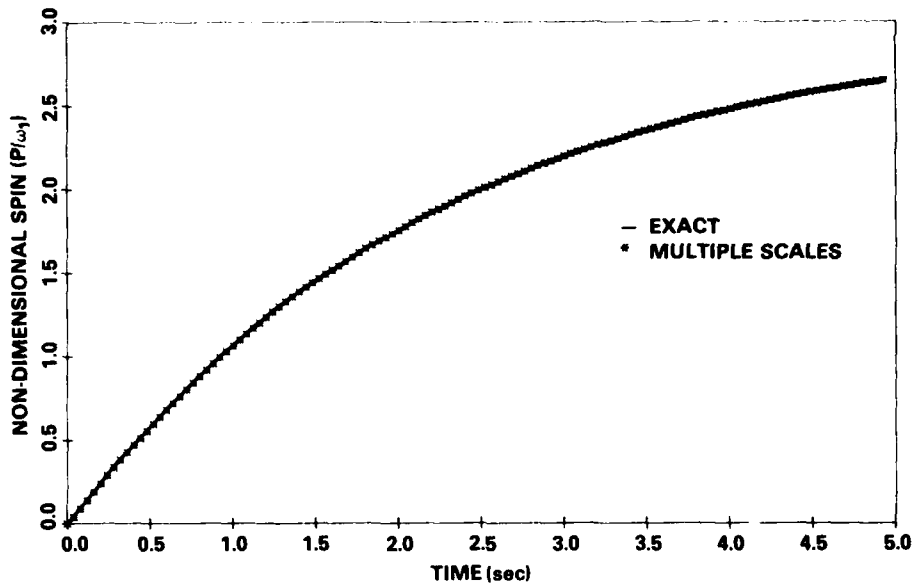


Figure 12. - Missile Induced Rolling Motion - Passage Through Resonance
 $(k_1 = 0.11, k_2 = 0, \alpha_T = 6.3^\circ)$

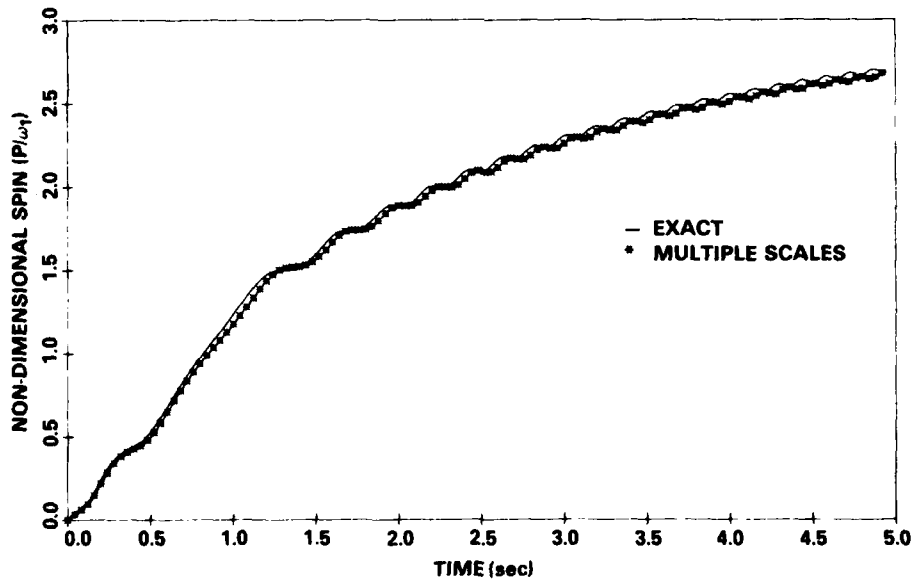


Figure 13. - Missile Induced Rolling Motion - Passage Through Resonance
 $(k_1 = 0.21, k_2 = 0, \alpha_T = 12.0^\circ)$

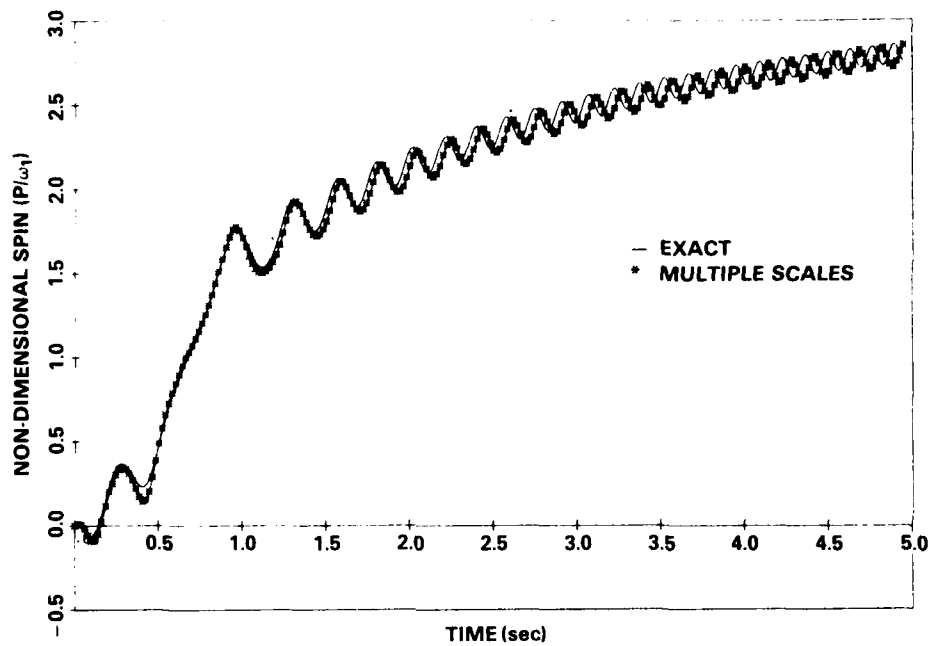


Figure 14. - Missile Induced Rolling Motion - Passage Through Resonance
 $(k_1 = 0.31, k_2 = 0, \alpha_T = 17.8^\circ)$

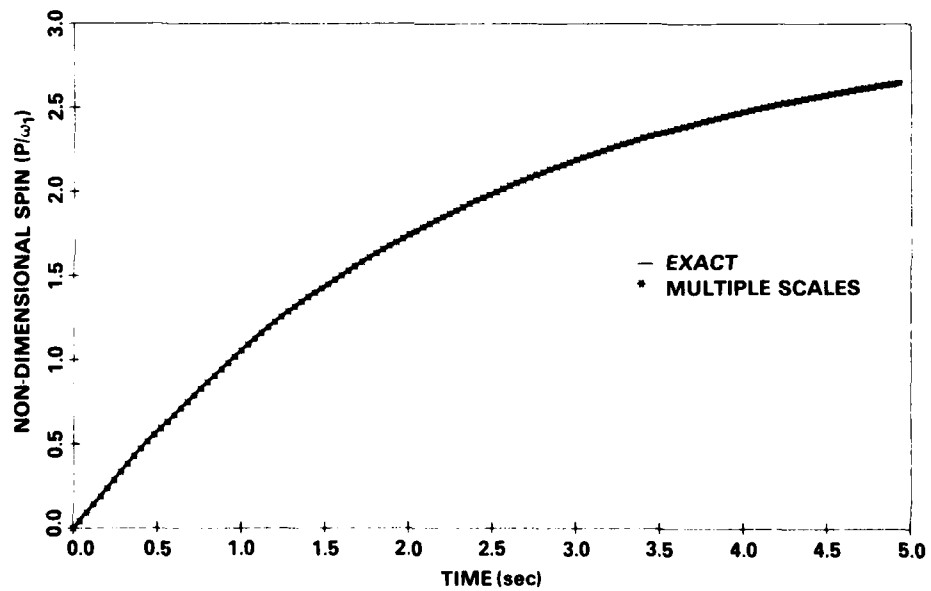


Figure 15. - Missile Induced Rolling Motion - Passage Through Resonance
 $(k_1 = 0.11, k_2 = 0.02, \alpha_T = 7.5^\circ)$

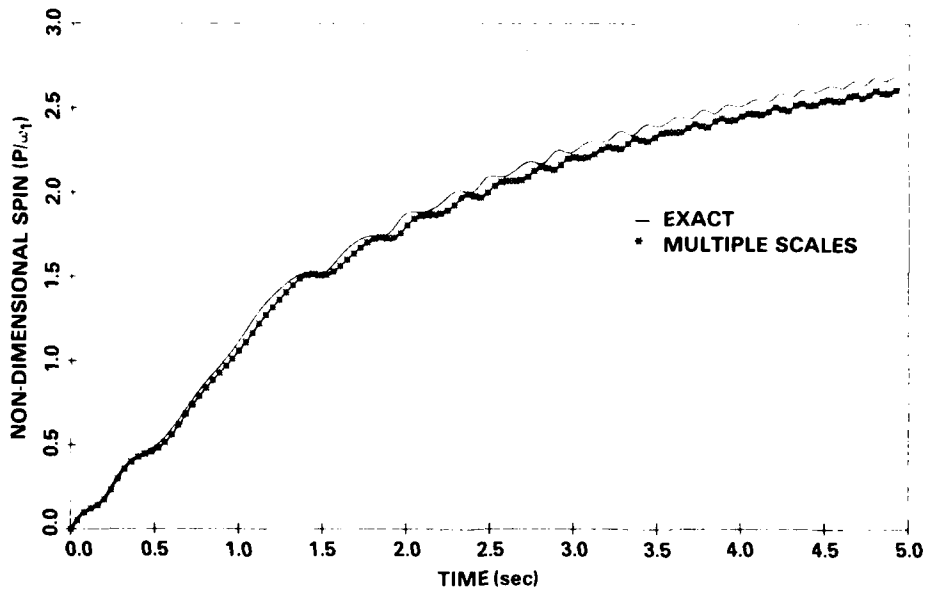


Figure 16. - Missile Induced Rolling Motion - Passage Through Resonance
 $(k_1 = 0.21, k_2 = 0.02, \alpha_T = 13.2^\circ)$

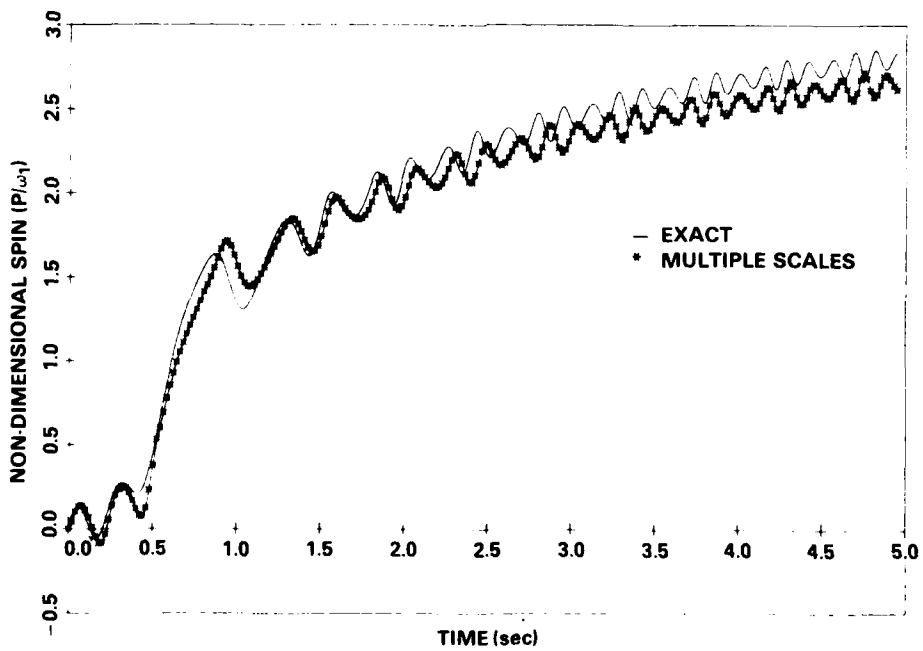


Figure 17. - Missile Induced Rolling Motion - Passage Through Resonance
 $(k_1 = 0.31, k_2 = 0.04, \alpha_T = 20.1^\circ)$

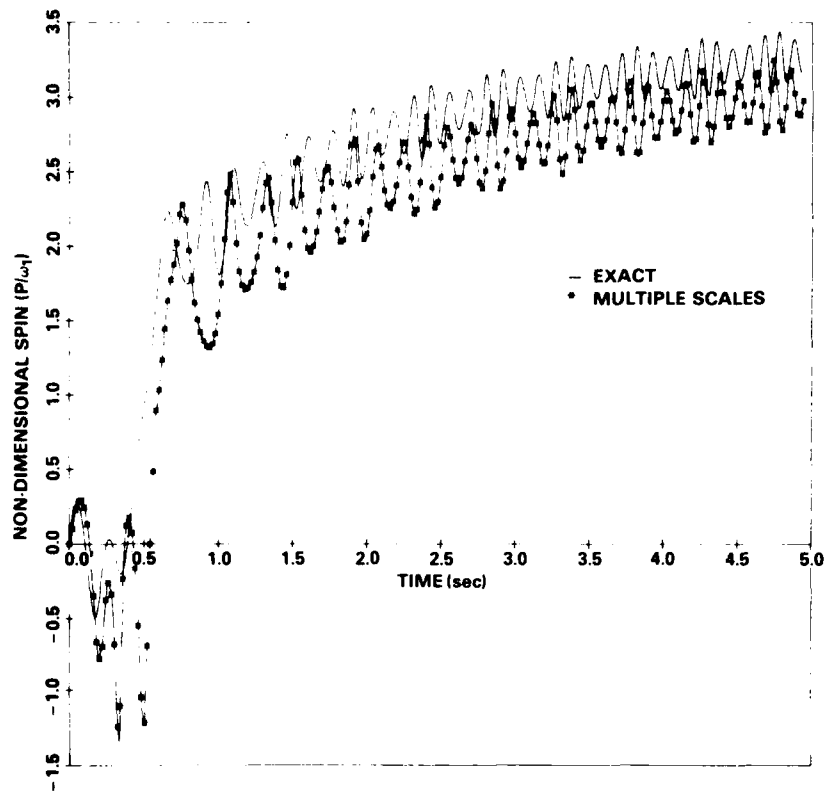


Figure 18. - Missile Induced Rolling Motion - Passage Through Resonance
 $(k_1 = 0.41, k_2 = 0.05, \alpha_T = 26.4^\circ)$

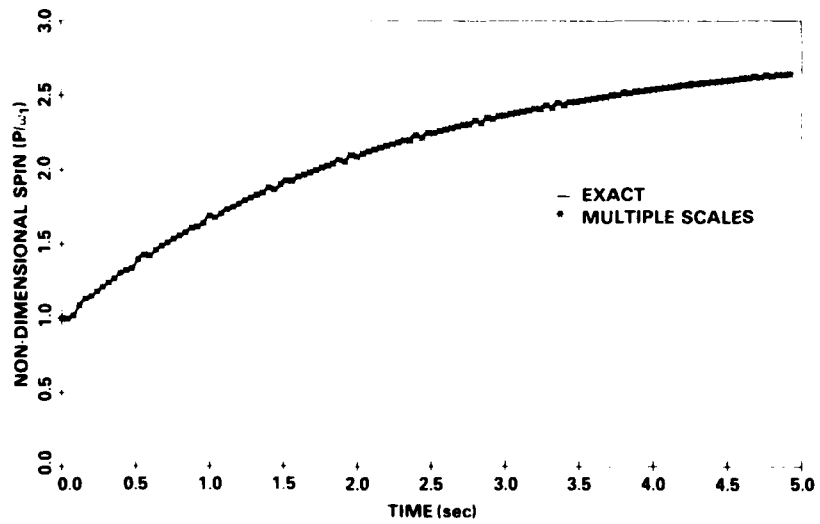


Figure 19. - Missile Roll Rate History ($k_1 = 0.1, k_2 = 0.2, \alpha_T = 13.2^\circ$)

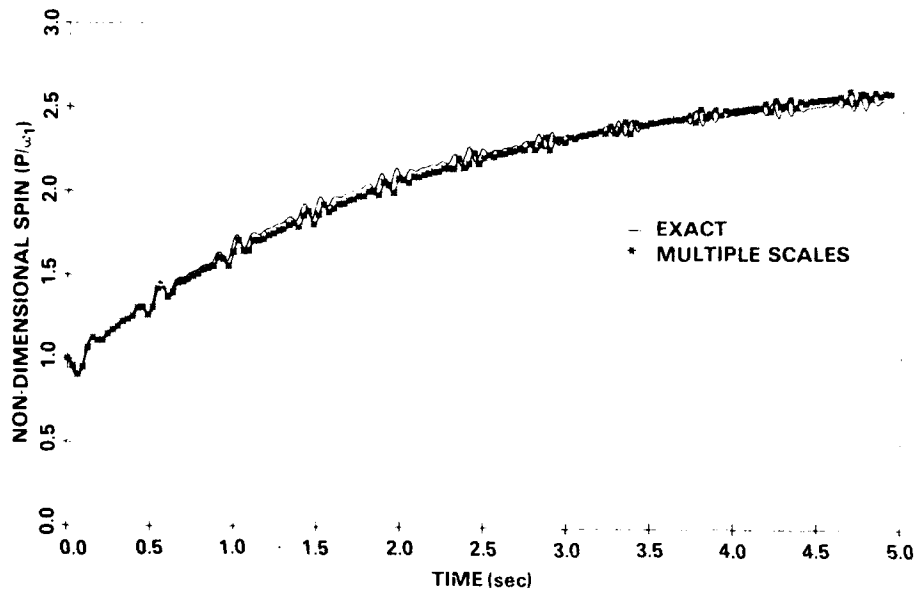


Figure 20. -- Missile Roll Rate History ($k_1 = 0.1, k_2 = 0.3, \alpha_T = 22.9^\circ$)

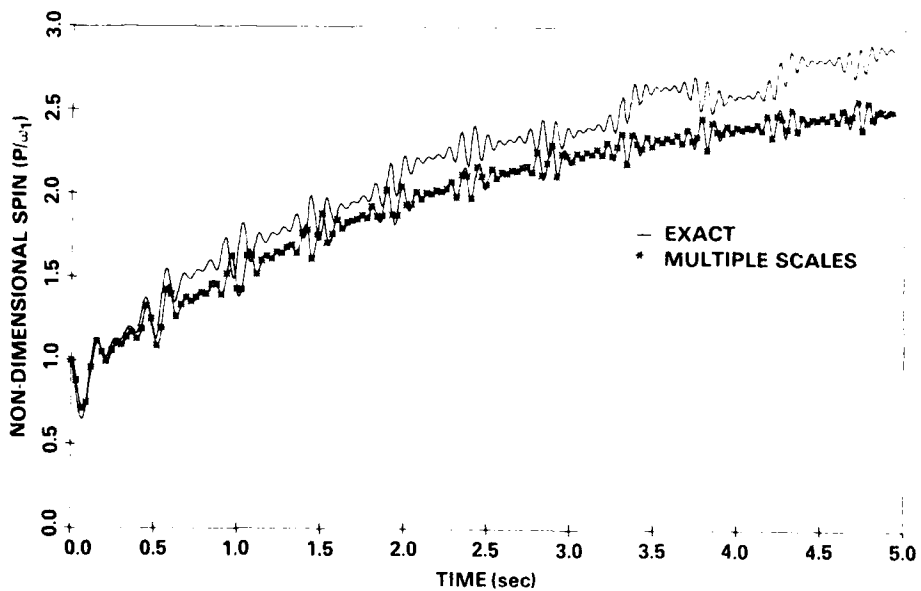


Figure 21. -- Missile Roll Rate History ($k_1 = 0.10, k_2 = 0.4, \alpha_T = 28.6^\circ$)

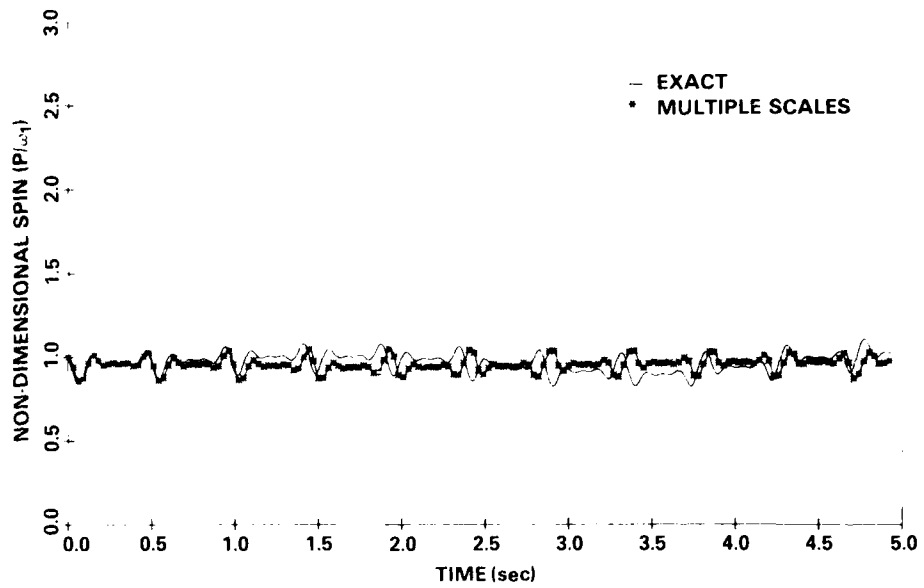


Figure 22. - Missile Roll Rate History ($k_1 = 0.10, k_2 = 0.30, \alpha_T = 22.9^\circ$)

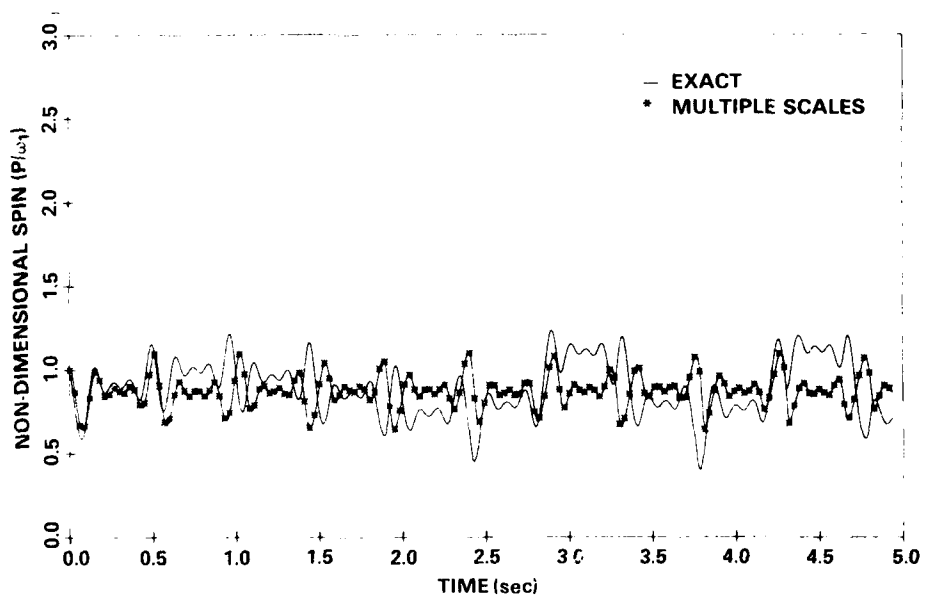


Figure 23. - Missile Roll Rate History ($k_1 = 0.10, k_2 = 0.40, \alpha_T = 28.6^\circ$)

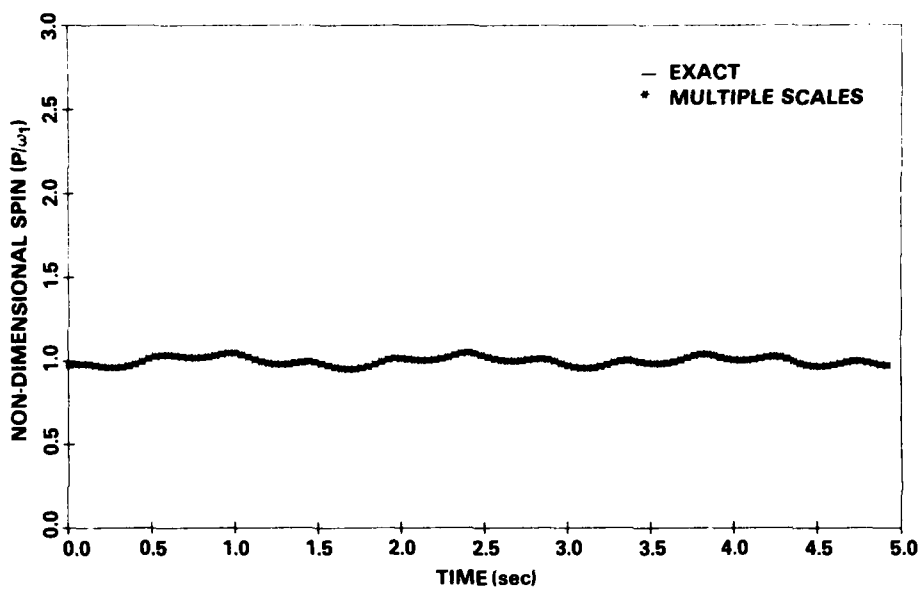


Figure 24. - Missile Roll Rate History ($k_1 = 0.21, k_2 = 0.02, \alpha_T = 13.2^\circ$)

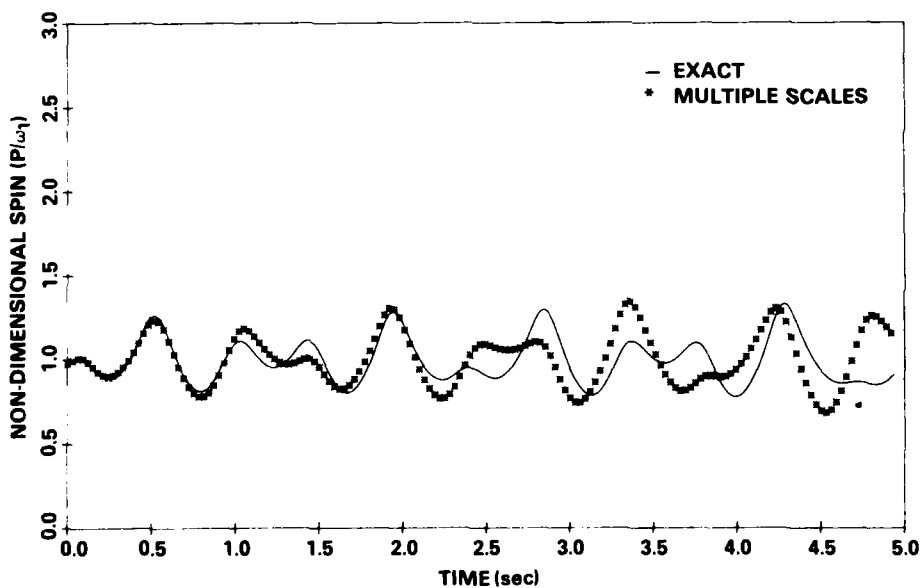


Figure 25. - Missile Roll Rate History ($k_1 = 0.31, k_2 = 0.02, \alpha_T = 19.5^\circ$)

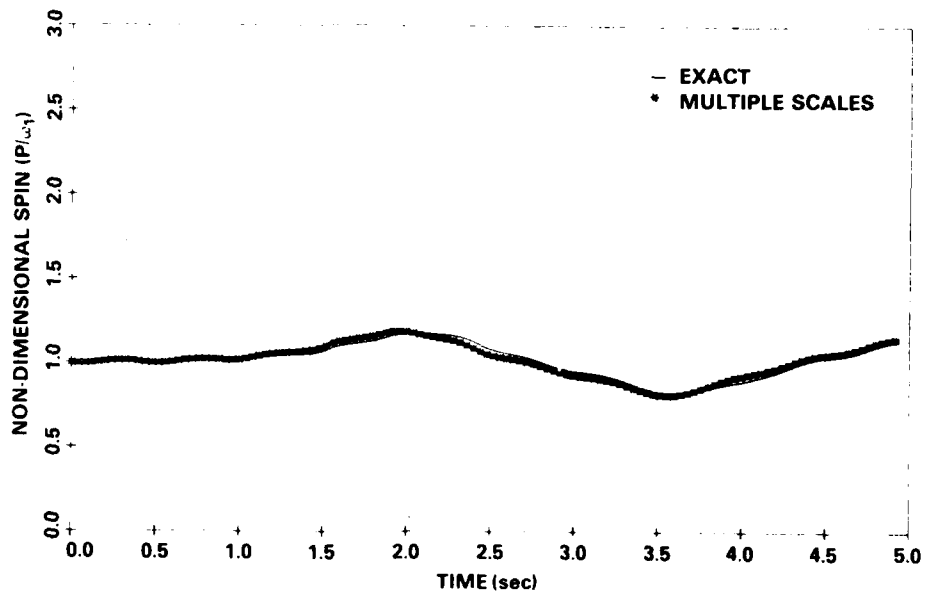


Figure 26. - Missile Roll Rate History ($k_1 = 0.21$, $k_2 = 0.02$, $\alpha_T = 13.2^\circ$)

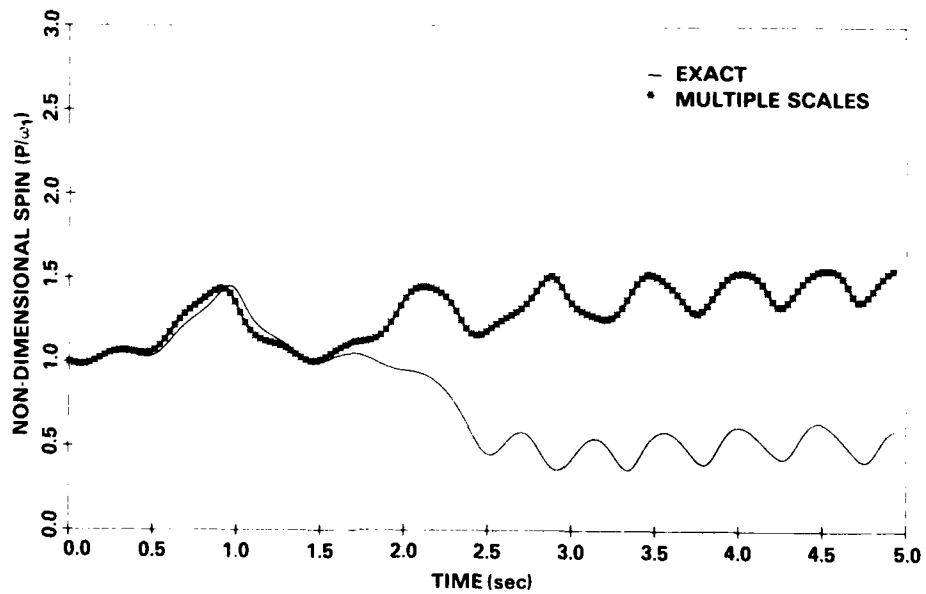


Figure 27. - Missile Roll Rate History ($k_1 = 0.31$, $k_2 = 0.03$, $\alpha_T = 19.5^\circ$)

CHAPTER V

COMBINED ROLL-YAW INTERACTION

The results of the preceding chapters have been instrumental in providing quantitative insight into the mechanisms of resonance instability as related to the effects of roll orientation-dependent aerodynamics. In addition, stability criteria useful to the designer have surfaced as a by-product of approximate solutions generated by the perturbation methods. While the two specific conditions studied, i.e., free yaw with prescribed rolling motion and induced rolling motion with prescribed yawing motion, have been instructive, neither can be considered totally representative of free-flight conditions. In this chapter, approximate solutions are sought which are representative of the full nonlinear problem of combined roll-yaw interaction.

The simultaneous differential equations governing the combined roll-yaw problem may be taken directly from Chapter III (Equation (3.1)) and Chapter IV (Equation (4.1))

$$\ddot{\xi} - iP_0\dot{\xi} - \omega_0^2\xi = \epsilon^2\mu_1\dot{\xi} + i\epsilon^2\mu_2\ddot{\xi} + \chi_1\delta^2e^{-i4\gamma\xi} \quad (5.1)$$

and

$$\dot{p} = \epsilon^4(\sigma_0 + \sigma_2p) + \text{Im}(\xi^4e^{-i4\phi}) \quad (5.2)$$

Note that the smallness parameter ϵ has been introduced into Equation (5.2) in a slightly different manner, such that terms on the right-hand side are of equal order of magnitude.

Approximate solutions to the system of nonlinear Equations (5.1) and (5.2) are again sought using a generalized version of the method of multiple scales similar to that of Chapter IV. It is assumed that ξ and p possess uniformly valid expansions of the form

$$\tilde{\xi}(t; \epsilon) = \epsilon\tilde{\xi}_1(\psi_1, \psi_2, T_2) + \epsilon^3\tilde{\xi}_3(\psi_1, \psi_2, \phi, T_2) + \dots \quad (5.3)$$

$$p(t; \epsilon) = p_0(T_4) + \epsilon^4p_4(\psi_1, \psi_2, \phi, T_4) + \dots$$

where

$$\frac{d\psi_j}{dt} = \omega_j, \quad (5.4)$$

and

$$T_j = \epsilon^j T_0 \quad (5.5)$$

The slow time scale T_2 is chosen so as to characterize the slowly varying nature of the modal amplitudes while the variable T_4 is introduced into the roll expansion in order to accommodate the comparatively slow variation of spin due to C_{ξ_0} . In addition, the assumed expansions of Equation (5.3) differ from previous expansions in that ξ may now exhibit roll dependence through the independent variable ϕ .

Equations (5.3) may now be substituted into Equations (5.1) and (5.2) to obtain partial differential equations in the independent variables ψ_j , T_j and ϕ . Equation (5.3) may be incorporated into Equation (5.2), equating all terms of order ϵ^4 to obtain

$$\omega_1 \frac{\partial p_4}{\partial \psi_1} + \omega_2 \frac{\partial p_4}{\partial \psi_2} + p_0 \frac{\partial p_4}{\partial \phi} = \left[-\frac{dp_0}{dT_4} + \sigma_0 + \sigma_2 p_0 \right] + \sigma_1 \text{Im}(\tilde{\xi}_1^4 e^{-i4\phi}) \quad (5.6)$$

Equation (5.6) is identical to the roll partial differential equation which resulted from the analysis of Chapter IV with the exception of the fact that $\tilde{\xi}_1$ is no longer constrained to be epicyclic with constant amplitudes and frequencies but may vary in accordance with Equation (5.1).

Equation (5.3) may be substituted into Equation (5.1) and terms of order ϵ and ϵ^3 equated to obtain partial differential equations for the solution of $\tilde{\xi}_1$ and $\tilde{\xi}_3$.

Terms $O(\epsilon)$:

$$\mathcal{L}^2(\tilde{\xi}_1) - iP_0 \mathcal{L}(\tilde{\xi}_1) - \omega_0^2 \tilde{\xi}_1 = 0 \quad (5.7)$$

Terms $O(\epsilon^3)$:

$$\begin{aligned} \mathcal{L}^2(\tilde{\xi}_3) - iP_0 \mathcal{L}(\tilde{\xi}_3) - \omega_0^2 \tilde{\xi}_3 = & -2\omega_1 \frac{\partial^2 \tilde{\xi}_1}{\partial \psi_1 \partial T_2} - 2\omega_2 \frac{\partial^2 \tilde{\xi}_1}{\partial \psi_2 \partial T_2} - \frac{d\omega_1}{dT_2} \frac{\partial \tilde{\xi}_1}{\partial \psi_1} - \frac{d\omega_2}{dT_2} \frac{\partial \tilde{\xi}_1}{\partial \psi_2} \\ & + iP_0 \frac{\partial \tilde{\xi}_1}{\partial T_2} + \mu_1 \mathcal{L}(\tilde{\xi}_1) + i\mu_2 \tilde{\xi}_1 + \chi_1 \tilde{\xi}_1^3 e^{i4\phi} \end{aligned} \quad (5.8)$$

where

$$\mathcal{L} = \omega_1 \frac{\partial}{\partial \psi_1} + \omega_2 \frac{\partial}{\partial \psi_2} \quad (5.9)$$

and the epicyclic frequencies ω_j are taken to be functions of slow time T_2 , to characterize the slow variation of the ω_j with mach number, dynamic pressure, etc. Thus Equations (5.6) through (5.9) represent the governing equations for $\tilde{\xi}_1$, p_0 , $\tilde{\xi}_3$, and p_4 .

A. NONRESONANT SOLUTIONS

The general solution to the homogeneous Equation (5.7) has the usual epicyclic form and may be written directly as

$$\tilde{\xi}_1 = \sum_{j=1}^2 K_j(T_2) e^{i\psi_j} \quad (5.10)$$

where

$$K_j = k_j e^{i\theta_j} \quad (5.11)$$

and

$$\psi_j = \omega_j T_0 \quad (5.12)$$

Equation (5.10) may be substituted into Equation (5.8) to obtain the partial differential equation governing $\tilde{\xi}_3$ resulting in

$$\mathcal{L}^2(\tilde{\xi}_3) - iP_0\mathcal{L}(\tilde{\xi}_3) - \omega_0^2\tilde{\xi}_3 = w_1e^{i\psi_1} + w_2e^{i\psi_2} + \chi_1\left[\bar{K}_1^3e^{i(4\phi-3\psi_1)} + \bar{K}_2^3e^{i(4\phi-3\psi_2)} + 3\bar{K}_1^2\bar{K}_2e^{i(4\phi-2\psi_1-\psi_2)} + 3\bar{K}_1\bar{K}_2^2e^{i(4\phi-\psi_1-2\psi_2)}\right] \quad (5.13)$$

where

$$w_1 = i(P_0 - 2\omega_1) \frac{dK_1}{dT_2} + i\left(\mu_1\omega_1 + \mu_2 - \frac{d\omega_1}{dT_2}\right)K_1 \quad (5.14)$$

and

$$w_2 = i(P_0 - 2\omega_2) \frac{dK_2}{dT_2} + i\left(\mu_1\omega_2 + \mu_2 - \frac{d\omega_2}{dT_2}\right)K_2 \quad (5.15)$$

In order to obtain a uniformly valid solution to Equation (5.13) that remains bounded as $T_0 \rightarrow \infty$, it is required that the secular terms vanish ($w_1 = w_2 = 0$), which results in the differential equations characterizing the slowly varying K_j 's

$$i(P_0 - 2\omega_1) \frac{dK_1}{dT_2} + i\left(\mu_1\omega_1 + \mu_2 - \frac{d\omega_1}{dT_2}\right)K_1 = 0 \quad (5.16)$$

$$i(P_0 - 2\omega_2) \frac{dK_2}{dT_2} + i\left(\mu_1\omega_2 + \mu_2 - \frac{d\omega_2}{dT_2}\right)K_2 = 0. \quad (5.17)$$

With these secular terms removed, the particular solution to Equation (5.13) becomes

$$\tilde{\xi}_3 = \alpha_1e^{i(4\phi-3\psi_1)} + \alpha_2e^{i(4\phi-3\psi_2)} + \alpha_3e^{i(4\phi-2\psi_1-\psi_2)} + \alpha_4e^{i(4\phi-\psi_1-2\psi_2)} \quad (5.18)$$

where

$$\alpha_1 = \frac{-\chi_1\bar{K}_1^3}{(4p_0 - 3\omega_1)^2 - P_0(4p_0 - 3\omega_1) + \omega_0^2}$$

$$\alpha_2 = \frac{-\chi_1\bar{K}_2^3}{(4p_0 - 3\omega_2)^2 - P_0(4p_0 - 3\omega_2) + \omega_0^2} \quad (5.19)$$

$$\alpha_3 = \frac{-3\chi_1\bar{K}_1^2\bar{K}_2}{(4p_0 - 2\omega_1 - \omega_2)^2 - P_0(4p_0 - 2\omega_1 - \omega_2) + \omega_0^2}$$

and

$$\alpha_4 = \frac{-3\chi_1\bar{K}_1\bar{K}_2^2}{(4p_0 - \omega_1 - 2\omega_2)^2 - P_0(4p_0 - \omega_1 - 2\omega_2) + \omega_0^2}$$

Returning to the differential equation of rolling motion, Equation (5.10) may be substituted into Equation (5.6), and again eliminating the secular term, the slow variation of $p_0(T_4)$ is given by

$$-\frac{dp_0}{dT_4} + \sigma_0 + \sigma_2 p_0 = 0 \quad (5.20)$$

The particular solution to Equation (5.6), with the secular term removed, may then be written

$$p_4(t) = \beta_1 \cos 4(\hat{\psi}_1 - \phi) + \beta_2 \cos 4(\hat{\psi}_2 - \phi) + \beta_3 \cos(3\hat{\psi}_1 + \hat{\psi}_2 - 4\phi) \\ + \beta_4 \cos 2(\hat{\psi}_1 + \hat{\psi}_2 - 2\phi) + \beta_5 \cos(\hat{\psi}_1 + 3\hat{\psi}_2 - 4\phi) \quad (5.21)$$

with

$$\beta_1 = \frac{\sigma_1 k_1^4}{4(p_0 - \omega_1)} \\ \beta_2 = \frac{\sigma_1 k_2^4}{4(p_0 - \omega_2)} \quad (5.22) \\ \beta_3 = \frac{4\sigma_1 k_1^3 k_2}{4p_0 - 3\omega_1 - \omega_2} \\ \beta_4 = \frac{3\sigma_1 k_1^2 k_2^2}{2p_0 - \omega_1 - \omega_2} \\ \beta_5 = \frac{4\sigma_1 k_1 k_2^3}{4p_0 - \omega_1 - 3\omega_2}$$

and

$$\hat{\psi}_j = \omega_j T_0 + \theta_j \quad (5.23)$$

Inspection of Equations (5.10) through (5.23), which constitute the first and second approximate solutions for $p(t)$ and $\xi(t)$, reveals that the full problem of combined roll-yaw interaction may be treated as a superposition of the two previously treated problems, so long as the assumptions regarding the perturbation nature of the problem remain valid.

B. RESONANT SOLUTIONS

Similar to the behavior investigated in Chapters III and IV, the higher-order approximate solutions for coupled yawing and rolling motion, (ξ_3, p_4) , become singular as the roll rate approaches the distinct values of zero spin, resonance ($p = \omega_1$) and approximately one-half resonant spin. This difficulty is evidenced by the singular behavior of the terms of Equations (5.19) and (5.22) as p_0 approaches one of these critical roll rates. Further evidence may be

obtained through an observation of the nonhomogeneous terms of Equations (5.6) and (5.13) as the roll rate approaches the above critical values. Selected high frequency terms become stationary or, at best, are slowly varying functions of time (T_2, T_4), which give rise to secular terms in the expansions for p and ξ . Perturbation solutions which are valid in the vicinity of these singular roll rates must be generated individually and these solutions "matched" to obtain continuous approximate representation of the motion. Solutions valid in the vicinity of resonance are generated in what follows. For the sake of brevity, derivation of solutions valid at $p_0 = 0$, $(3\omega_1 + \omega_2)/4$ are omitted but may be easily derived in a manner similar to the case of resonant spin, $p = \omega_1$.

At resonance, the ψ_j and ϕ are interpreted as $\omega_j T_0$ and $p_0 T_0$ respectively and Equation (5.13) may be rewritten, grouping stationary terms, as

$$\begin{aligned} \mathcal{L}^2(\tilde{\xi}_3) - iP_0 \mathcal{L}(\tilde{\xi}_3) - \omega_0^2 \tilde{\xi}_3 = & \left[w_1 + \chi_1 \bar{K}_1^3 e^{i4\phi_0} \right] e^{i\psi_1} + w_2 e^{i\psi_2} \\ & + \chi_1 \left[\bar{K}_2^3 e^{i(4\phi-3\psi_2)} + 3\bar{K}_1 \bar{K}_2^2 e^{i(4\phi-\psi_1-2\psi_2)} + 3\bar{K}_1^2 K_2 e^{i(4\phi-2\psi_1-\psi_2)} \right] \end{aligned} \quad (5.24)$$

In order for the solution to Equation (5.24) to remain uniformly valid, it is required that the secular terms vanish

$$w_1 + \chi_1 \bar{K}_1^3 e^{i4\phi_0} = 0 \quad (5.25)$$

$$w_2 = 0 \quad (5.26)$$

The solution of Equation (5.24), with secular terms removed, may now be obtained as:

$$\tilde{\xi}_3(t) = \alpha_2 e^{i(4\phi-3\psi_2)} + \alpha_3 e^{i(4\phi-2\psi_1-\psi_2)} + \alpha_4 e^{i(4\phi-\psi_1-2\psi_2)} \quad (5.27)$$

Thus the resulting asymptotic expansion for $\tilde{\xi}(t)$, valid at fundamental resonance, is written as

$$\tilde{\xi}(t; \epsilon) = \epsilon \tilde{\xi}_1(\psi_1, \psi_2, T_2) + \epsilon^3 \tilde{\xi}_3(\psi_1, \psi_2, \phi, T_4) \quad (5.28)$$

with $\tilde{\xi}_1$ and $\tilde{\xi}_3$ given by Equations (5.10) and (5.27) respectively.

The solution to the nonlinear rolling motion at resonance is generated by a consideration of Equation (5.6) as $p \rightarrow \omega_1$. Grouping stationary (slowly varying) terms, Equation (5.6) may be expanded and rewritten as:

$$\begin{aligned} \omega_1 \frac{\partial p_4}{\partial \psi_1} + \omega_2 \frac{\partial p_4}{\partial \psi_2} + p_0 \frac{\partial p_4}{\partial \phi} = & \left[-\frac{dp_0}{dT_4} + p_0 + \sigma_2 p_0 + \sigma_1 k_1^4 \sin 4(\theta_1 - \phi_0) \right] \\ & + \sigma_1 \left[k_2^4 \sin 4(\hat{\psi}_2 - \phi) + 4k_1^3 k_2 \sin(3\hat{\psi}_1 + \hat{\psi}_2 - 4\phi) \right. \\ & \left. + 6k_1^2 k_2^2 \sin 2(\hat{\psi}_1 + \hat{\psi}_2 - 2\phi) + 4k_1 k_2^3 \sin(\hat{\psi}_1 + 3\hat{\psi}_2 - 4\phi) \right] \end{aligned} \quad (5.29)$$

Elimination of the slowly-varying secular terms yields the governing equation for p_0 :

$$\frac{dp_0}{dT_4} = \sigma_0 + \sigma_2 p_0 + \sigma_1 k_1^4 \sin 4(\theta_1 - \phi_0) \quad (5.30)$$

The uniformly valid solution for p_4 is then solved for directly and is found to be:

$$p_4(t) = \beta_2 \cos 4(\hat{\psi}_2 - \phi) + \beta_3 \cos(3\hat{\psi}_1 + \hat{\psi}_2 - 4\phi) \\ + \beta_4 \cos 2(\hat{\psi}_1 + \hat{\psi}_2 - 2\phi) + \beta_5 \cos(\hat{\psi}_1 + 3\hat{\psi}_2 - 4\phi) \quad (5.31)$$

C. STABILITY AT RESONANCE

Equations (5.27) through (5.31) comprise approximate solutions to the combined roll-yaw motion valid in the vicinity of resonance. While these results contain considerable information regarding the character of the coupled motion at resonance, they are nonlinear, time-varying, coupled differential equations that yield little quantitative information without recourse to direct numerical integration. Additional insight into the stability of the motion, in close proximity to resonant spin may be gained through a small perturbation analysis of Equations (5.27) through (5.31).

Equation (5.25) may be expanded into real and imaginary components to yield the differential equations governing the slowly varying nutation amplitude and phase

$$\frac{dk_1}{dT_2} = - \left(\frac{\mu_1 \omega_1 + \mu_2 - \omega_1''}{P_0 - 2\omega_1} \right) k_1 - \frac{\chi_1 k_1^3}{P_0 - 2\omega_1} \sin 4(\phi - \hat{\psi}_1) \quad (5.32)$$

$$\frac{dp_0}{dT_2} = \frac{\chi_1 k_1^2}{P_0 - 2\omega_1} \cos 4(\phi - \hat{\psi}_1) \quad (5.33)$$

The governing differential equation of rolling motion at resonance is taken from Equation (5.30) as

$$\frac{dp_0}{dT_4} = \sigma_0 + \sigma_2 p_0 + \sigma_1 k_1^4 \sin 4(\phi - \hat{\psi}_1) \quad (5.34)$$

An investigation of the combined rolling and yawing motion in the neighborhood of $p_0 = \omega_1$ proceeds by considering the phase $\phi - \hat{\psi}_1$ to be essentially stationary, or at most a slowly varying function of T_2 at resonance. Allowable perturbations about resonance are made possible through the introduction of the detuning parameter λ , such that

$$P_0 = \omega_1 + \epsilon^2 \lambda \quad (5.35)$$

where λ is of order unity. Substitution of Equation (5.35) into Equations (5.32) through (5.34), with the interpretation of ψ_1 as $\omega_1 T_0$, yields the following nonlinear system

$$\frac{dk_1}{dT_2} = - \left(\frac{\mu_1 \omega_1 + \mu_2 - \omega_1''}{P_0 - 2\omega_1} \right) k_1 - \frac{\chi_1 k_1^3}{P_0 - 2\omega_1} \sin \Gamma \quad (5.36)$$

$$\frac{d\Gamma}{dT_2} = 4\lambda - \frac{4\chi_1}{P_0 - 2\omega_1} k_1^2 \cos \Gamma \quad (5.37)$$

$$\frac{d\lambda}{dT_2} = \sigma_1 k_1^4 \sin \Gamma \quad (5.38)$$

where

$$\Gamma \equiv 4(\phi_0 - \theta_1 + \lambda T_2) \quad (5.39)$$

and higher-order terms in ϵ have been neglected. Implicit in Equation (5.39) is the fact that $p_0 = \omega_1$ has been selected as the steady-state condition.

Stability of the motion at resonance can be analyzed by a small perturbation analysis of Equations (5.36) through (5.38) about the point $(k_0, \Gamma_0, 0)$ by introducing the perturbations

$$\left. \begin{aligned} k_1 &= k_0 + \hat{k} \\ \Gamma &= \Gamma_0 + \hat{\gamma} \end{aligned} \right\} \quad (5.40)$$

and expanding about $(k_0, \Gamma_0, 0)$ to yield the following perturbation equations

$$\frac{d\hat{k}}{dT_2} = (\eta_1 + 3\eta_2 \sin \Gamma_0)\hat{k} + (\eta_2 k_0^3 \cos \Gamma_0)\hat{\gamma} \quad (5.41)$$

$$\frac{d\hat{\gamma}}{dT_2} = 4\lambda - (8\eta_2 \cos \Gamma_0)\hat{k} + (4\eta_2 k_0^2 \sin \Gamma_0)\hat{\gamma} \quad (5.42)$$

$$\frac{d\lambda}{dT_2} = (4\sigma_1 \sin \Gamma_0)\hat{k} + (\sigma_1 k_0^4 \cos \Gamma_0)\hat{\gamma} \quad (5.43)$$

where

$$\eta_1 = - \left(\frac{\mu_1 \omega_1 + \mu_2 - \omega_1''}{P_0 - 2\omega_1} \right) \quad (5.44)$$

$$\eta_2 = - \frac{X_1}{P_0 - 2\omega_1} \quad (5.45)$$

Stability of this linear dynamic system is governed by the characteristic equation

$$\text{Det}(sI - A) = 0 \quad (5.46)$$

where

$$A = \begin{bmatrix} (\eta_1 - 3\eta_2 k_0^2 \sin \Gamma_0) & -(\eta_2 k_0^3 \cos \Gamma_0) & 0 \\ -(8\eta_2 k_0 \cos \Gamma_0) & (4\eta_2 k_0^2 \sin \Gamma_0) & 4 \\ 4\sigma_1 k_0^3 \sin \Gamma_0 & (\sigma_1 k_0^4 \cos \Gamma_0) & 0 \end{bmatrix} \quad (5.47)$$

The roots associated with the characteristic Equation (5.46) are shown graphically in Figures 28 through 32 for various values on nutation amplitude, k_1 . The root loci of Figures 28 through 31 indicate the possibility of

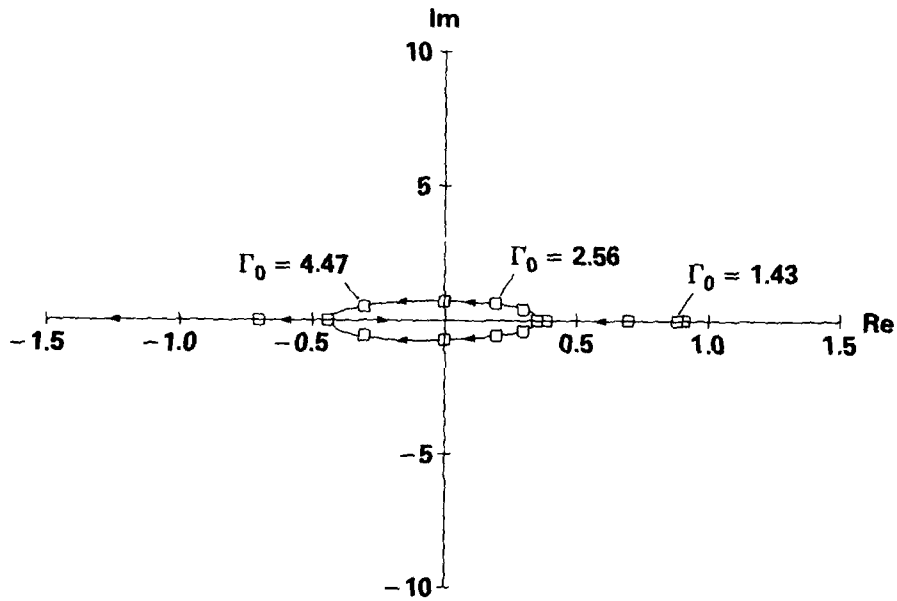


Figure 28. -- Root Locus at Resonance, $k_0 = 0.087$

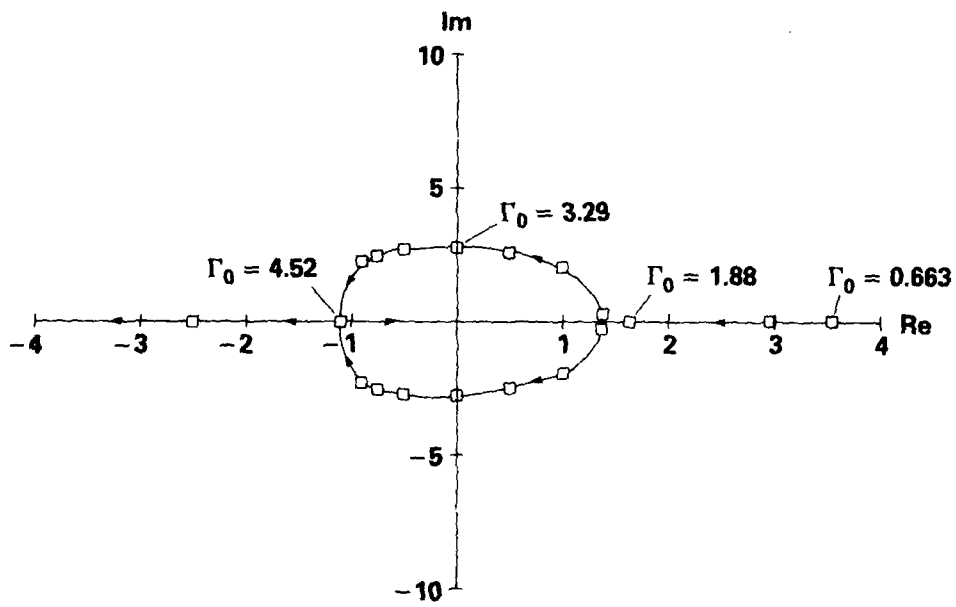


Figure 29. -- Root Locus at Resonance, $k_0 = 0.175$

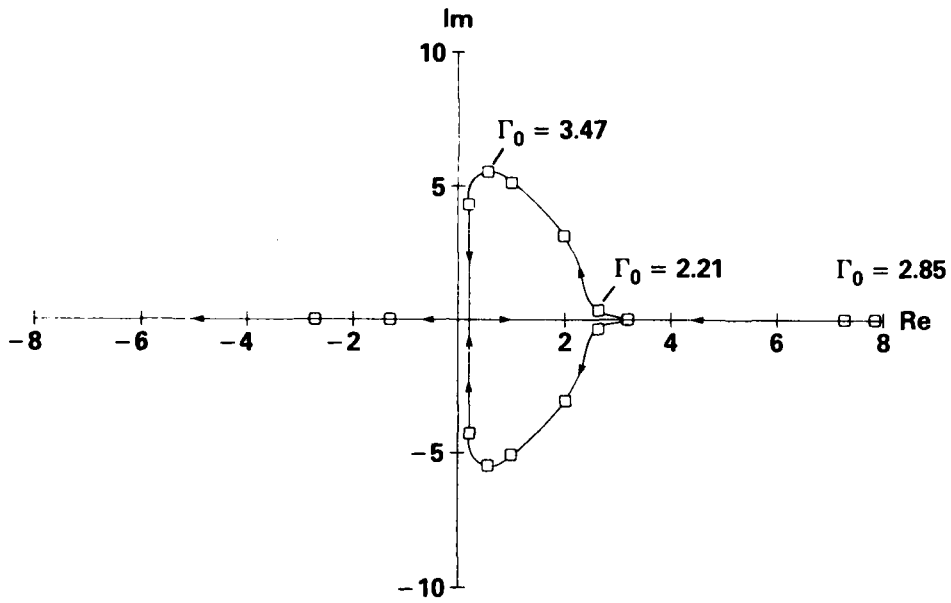


Figure 30. - Root Locus at Resonance, $k_0 = 0.262$

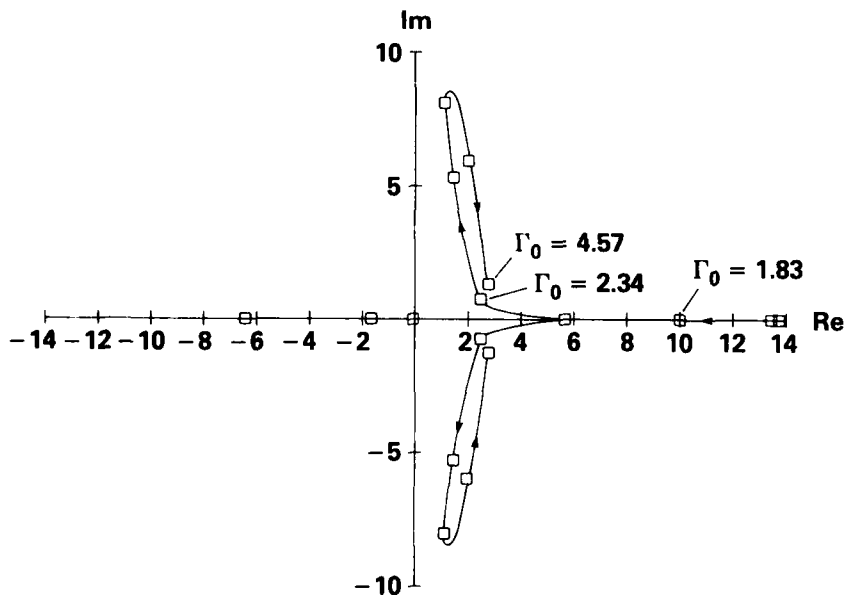


Figure 31. - Root Locus at Resonance, $k_0 = 0.349$

only mild instabilities associated with these roots with increasing frequency as the nutation amplitude increases. However, strongly divergent instabilities are possible due to a third real root, which may be large and positive.

The analytical results of Equation (5.46) were verified by direct numerical solutions of Equations (5.1) and (5.2) with the results shown graphically in Figures 33 through 38. Mild instabilities about resonance are depicted by the total angle of attack and roll rate histories in Figures 33 through 35 for various values of nutation amplitude. As the amplitude of the motion is increased, the mild oscillatory behavior of the nutation arm becomes more pronounced in agreement with the perturbation analysis.

The oscillatory behavior of the nutation amplitude associated with the solutions of Figures 33 through 35 is shown in Figure 36. Frequencies characteristic of this behavior are seen to be in agreement with the root loci of Figures 28 through 30. Note that the missile roll rate has departed significantly from its equilibrium value, $p = \omega_1$, where the perturbation assumption is no longer valid. In Figure 37, the missile stability in the vicinity of resonant spin is shown to be quite good for initial conditions producing small amplitude motion. In contrast, Figure 38 illustrates the sensitivity of the missile stability to small changes in initial conditions for large amplitudes motion. Note that although both solutions of Figure 38 have identical initial conditions, with the exception of small variations in Γ_0 , their angular motion and resultant spin rates are significantly different.

While not directly applicable to the small perturbation results, Figures 39 and 40 show total angle of attack and roll rate histories for configurations with fin cant with a resulting design roll rate of $3\omega_1$. The results of Figure 39 show stable missile angular motion when initial conditions are chosen in accordance with previous root loci predicting stable motion ($k_1 = 0.3$, $\Gamma_0 = 3.6$). The steady-state roll rate is seen to exponentially approach its design value with apparently little influence from the missile angular motion. However, when the initial phase angle Γ_0 is chosen such that the dominant real root of the linear perturbed system is large and positive, the divergent angular motion of Figure 40 is obtained together with a rapid divergence of the roll rate to a value well beyond the intended design value of $p_{ss} = 3\omega_1$. The critical value of spin producing the onset of magnus instability for this particular configuration was calculated to be $(p/\omega_1)_{crit} = 11.0$. The maximum roll rate produced by the resonance instability was approximately $(p/\omega_1)_{max} \approx 9.2$, just below that spin needed for magnus instability.

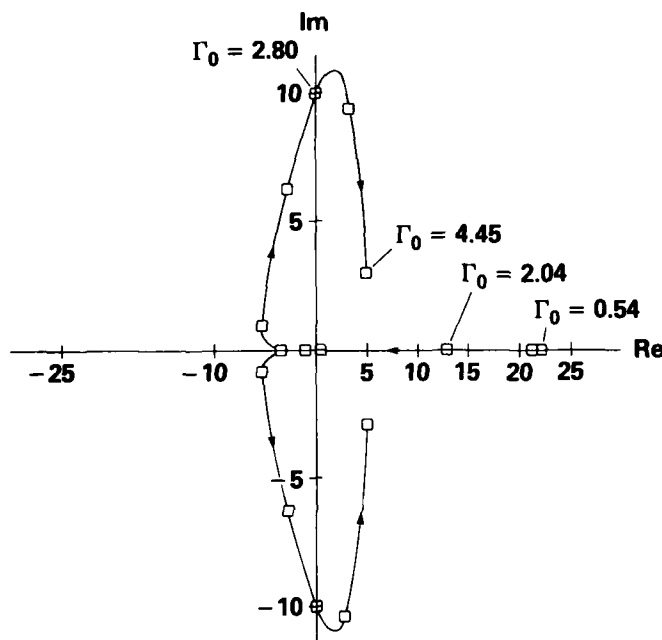


Figure 32. - Root Locus at Resonance, $k_0 = 0.436$

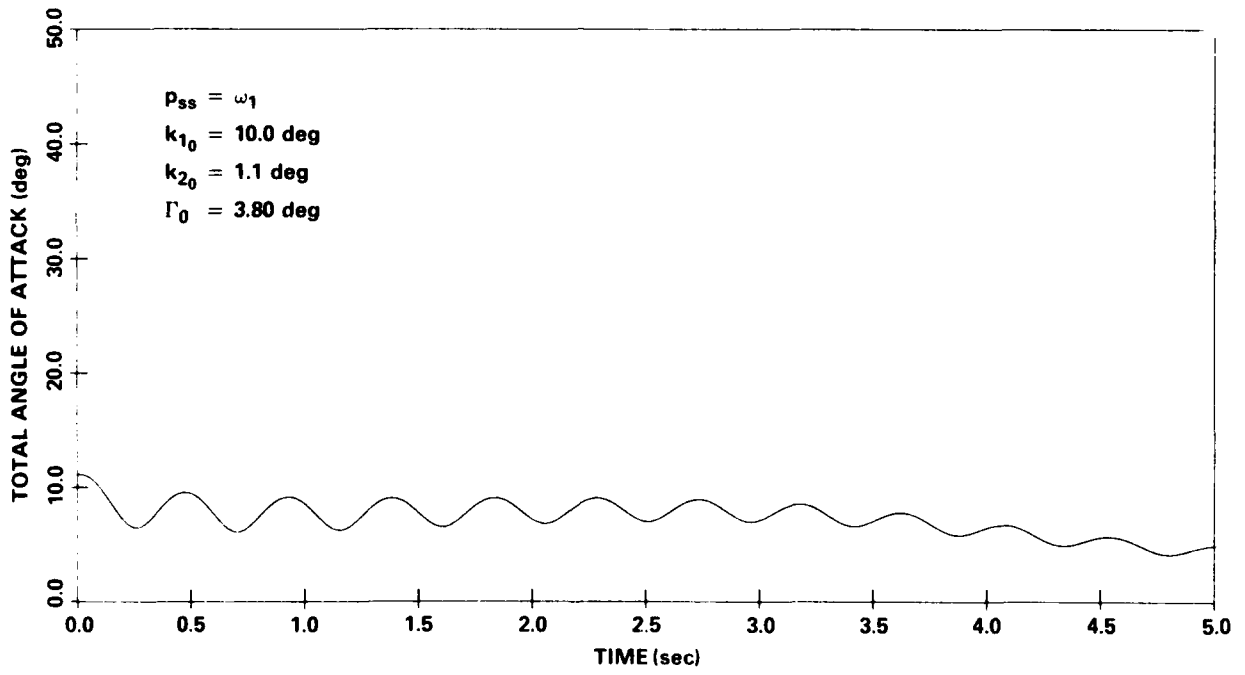
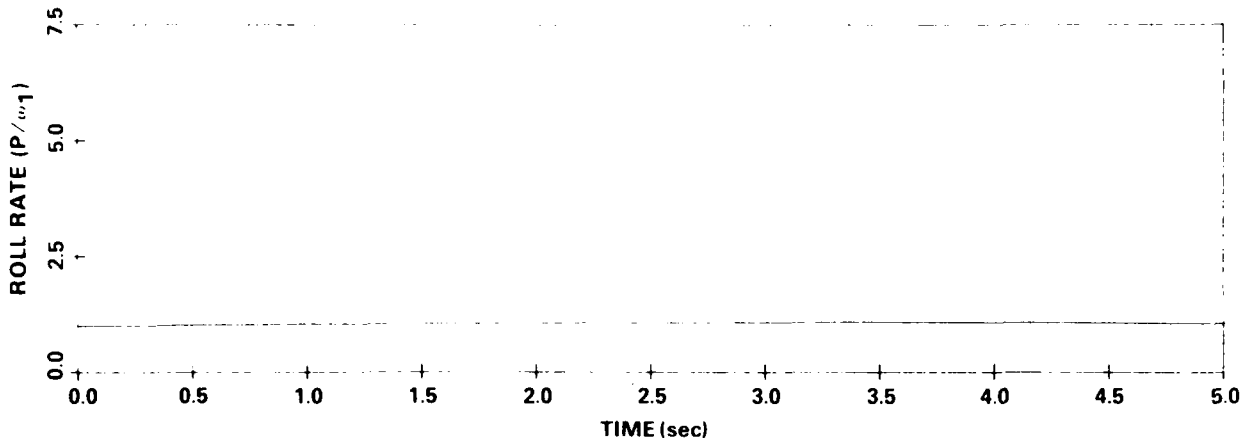


Figure 33. - Missile Stability at Resonance

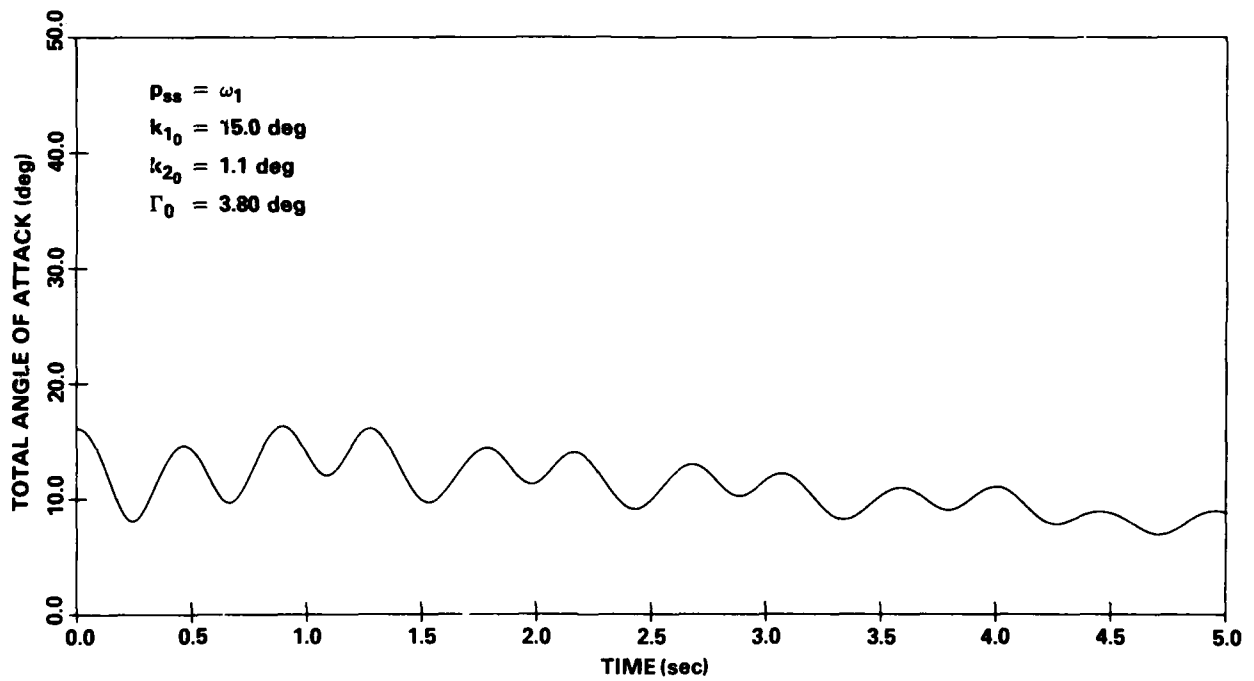
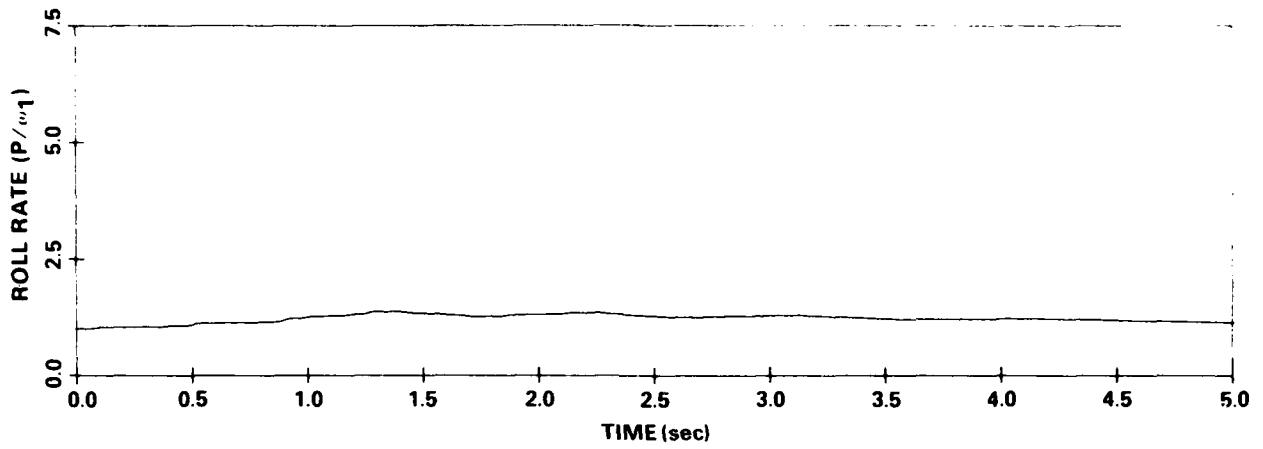


Figure 34. - Missile Stability at Resonance

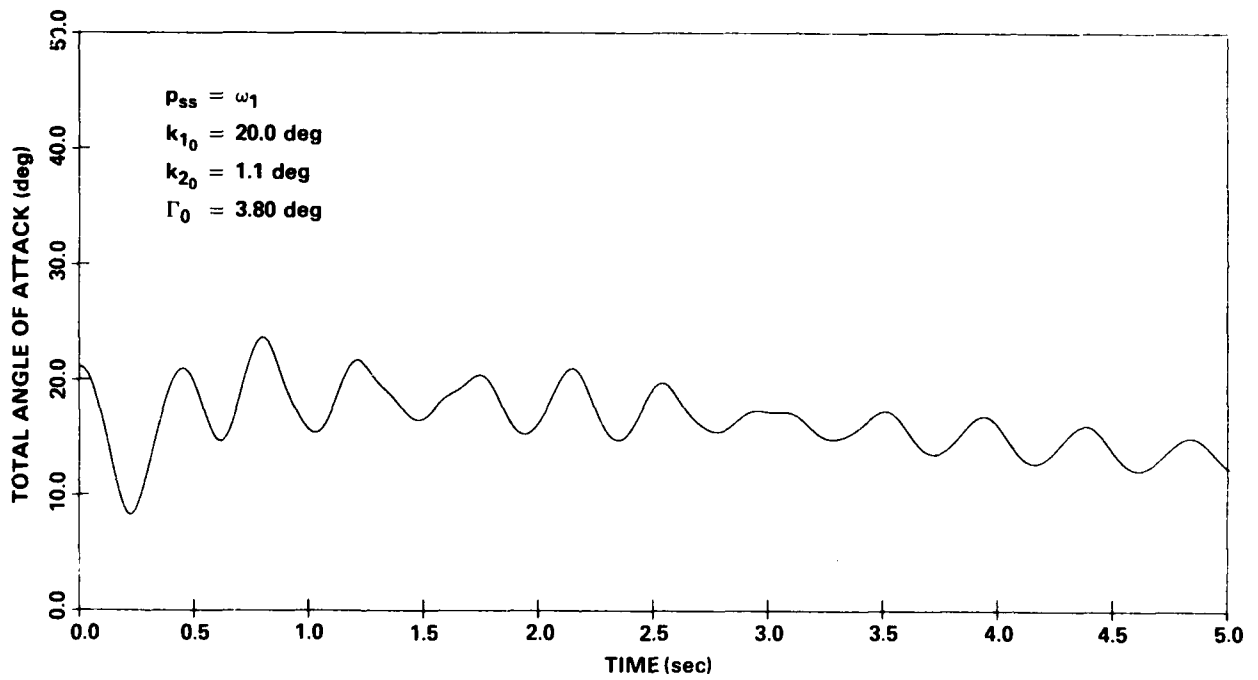
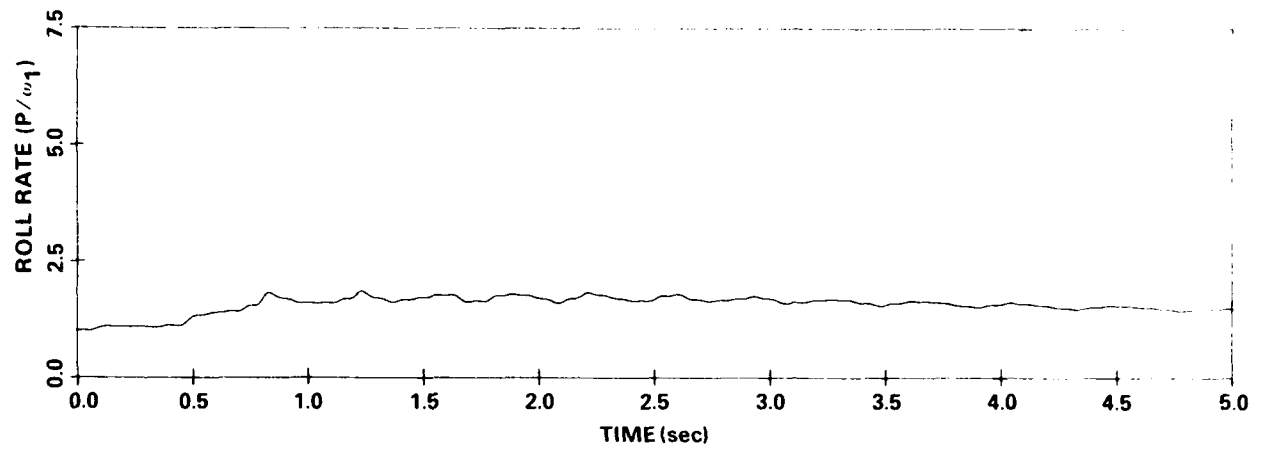


Figure 35. - Missile Stability at Resonance

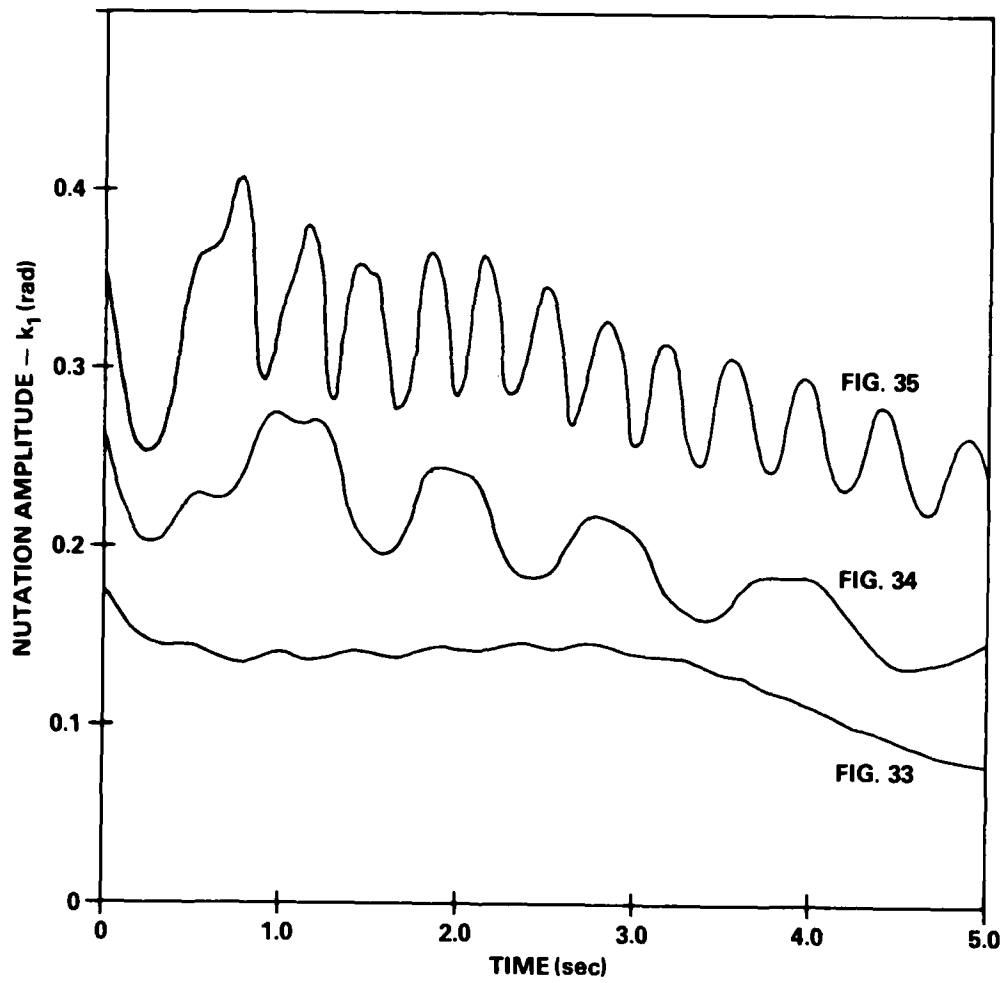


Figure 36. -Behavior of the Nutation Component at Various Amplitude Levels

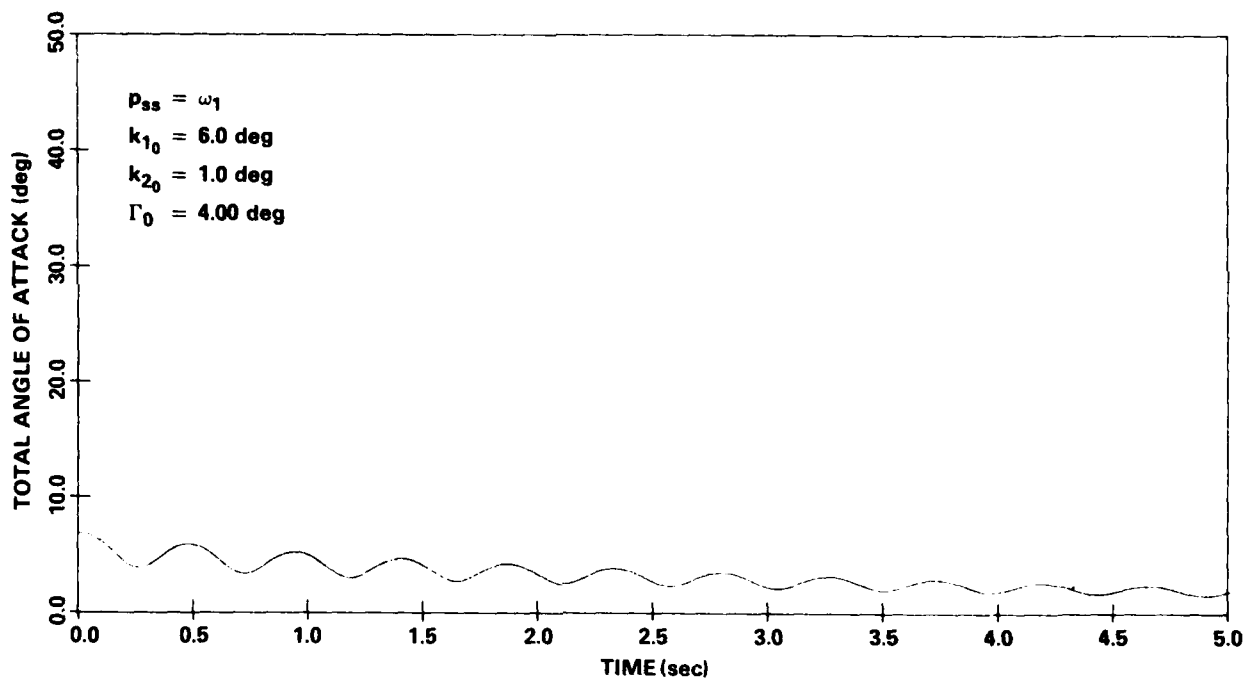
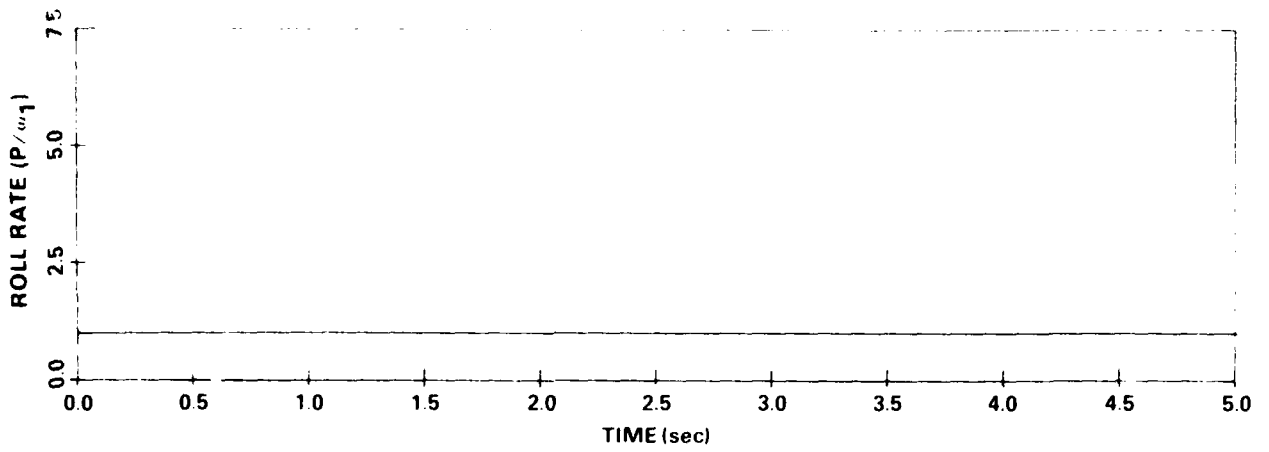


Figure 37. - Stable Angular Motion in the Vicinity of Resonant Spin

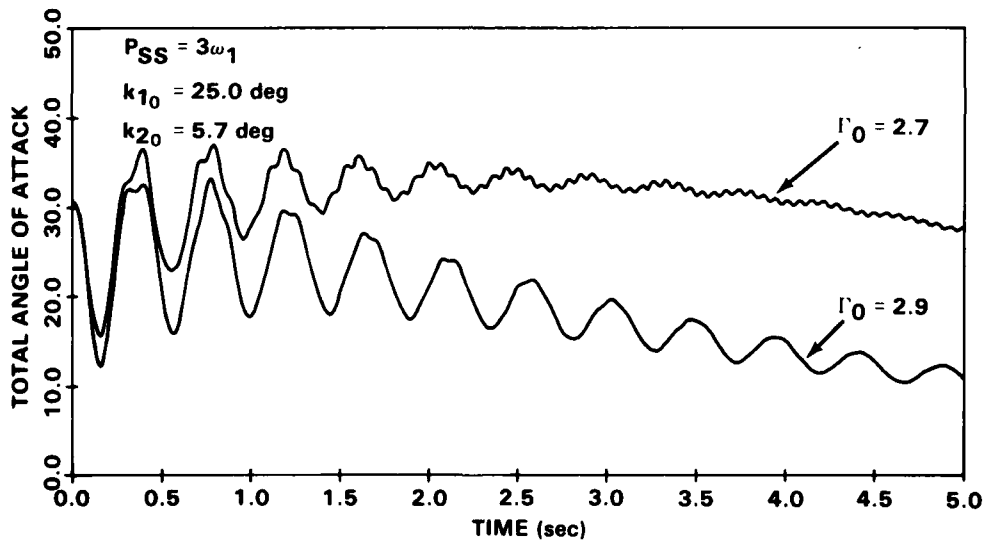
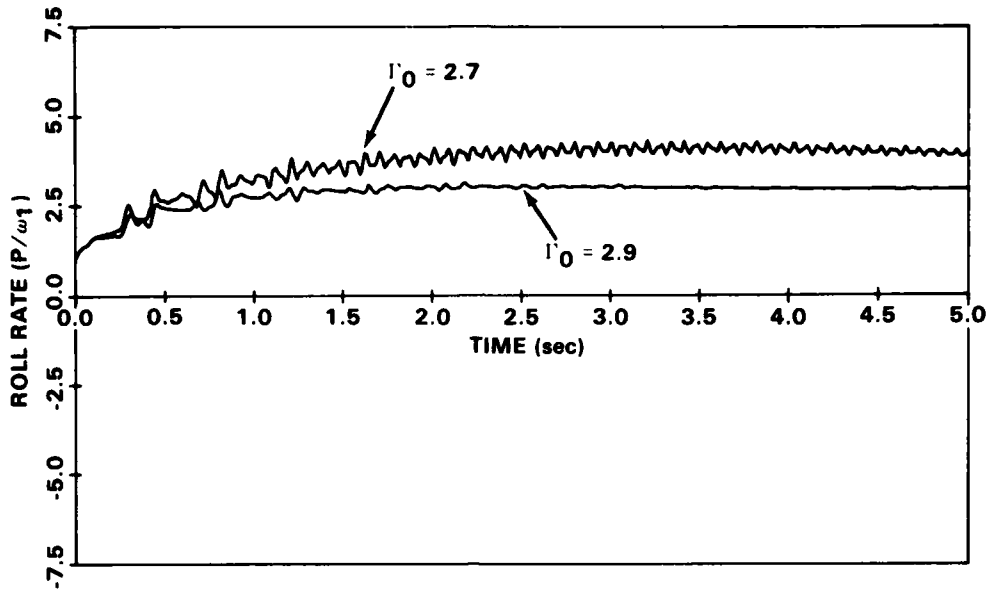


Figure 38.—Sensitivity to Initial Conditions
—Large Amplitude Motion

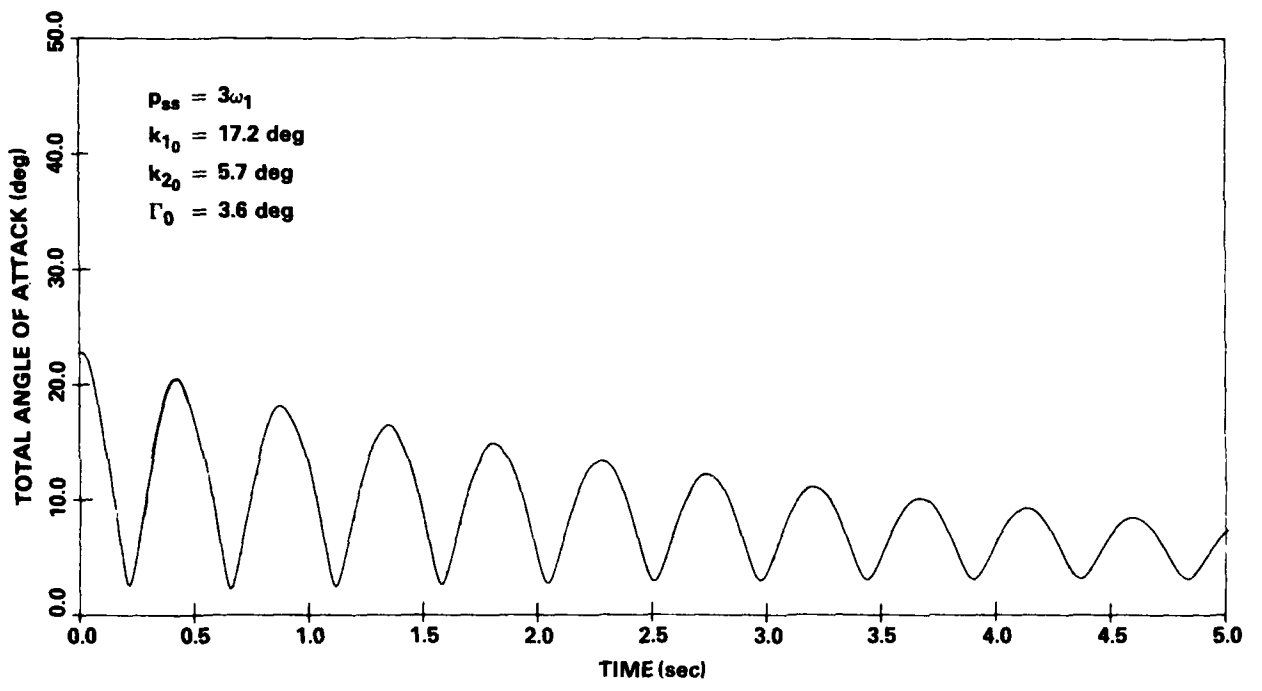
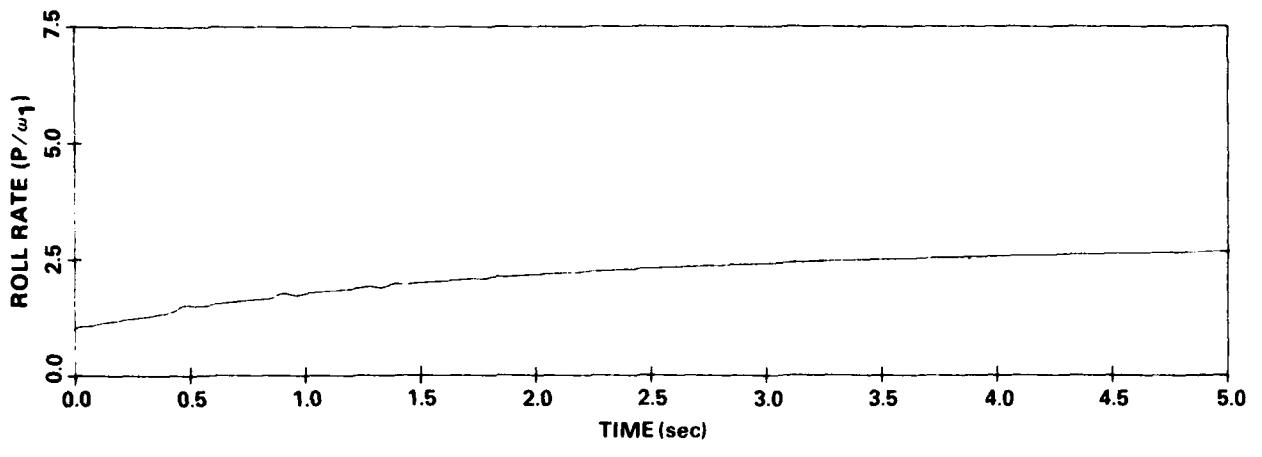


Figure 39. - Stable Passage Through Resonance

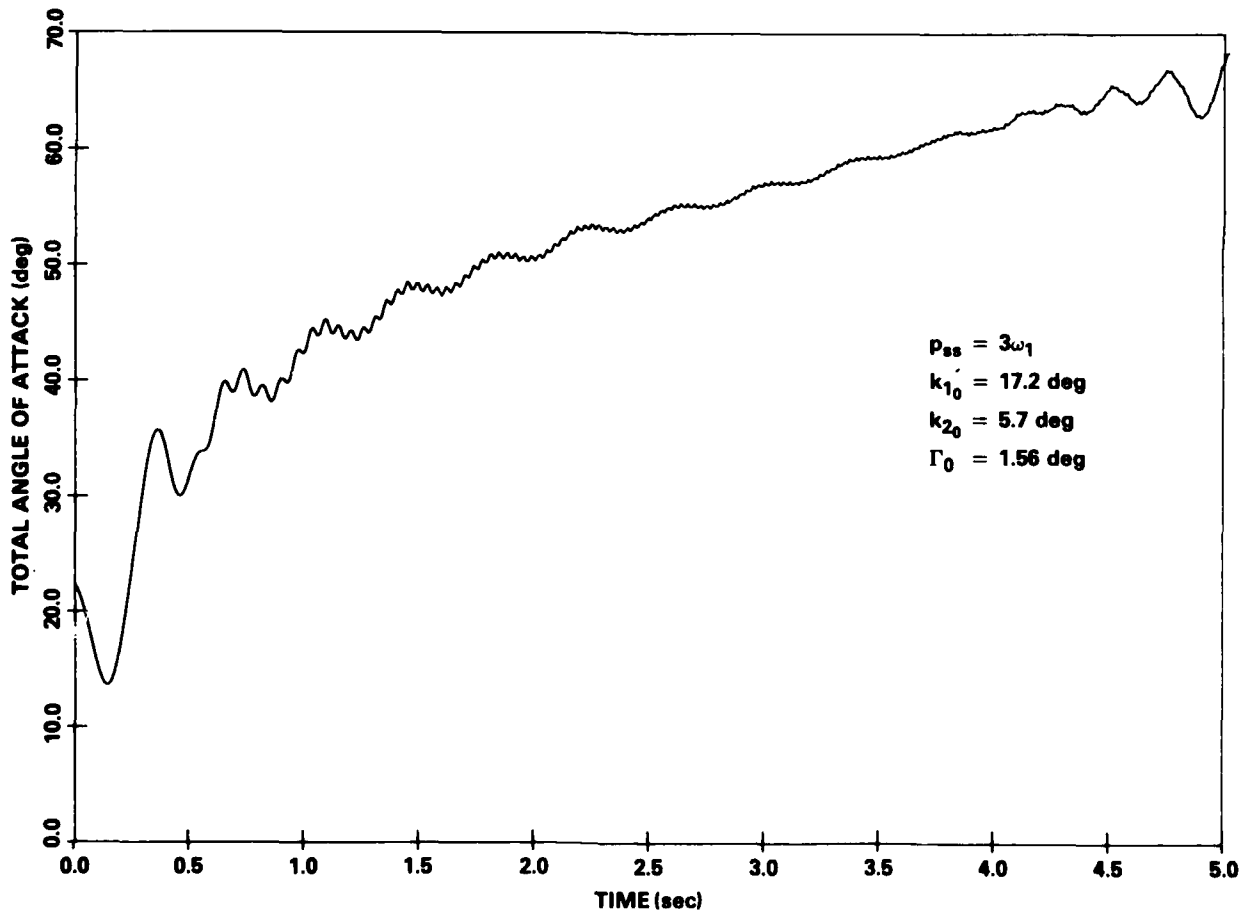
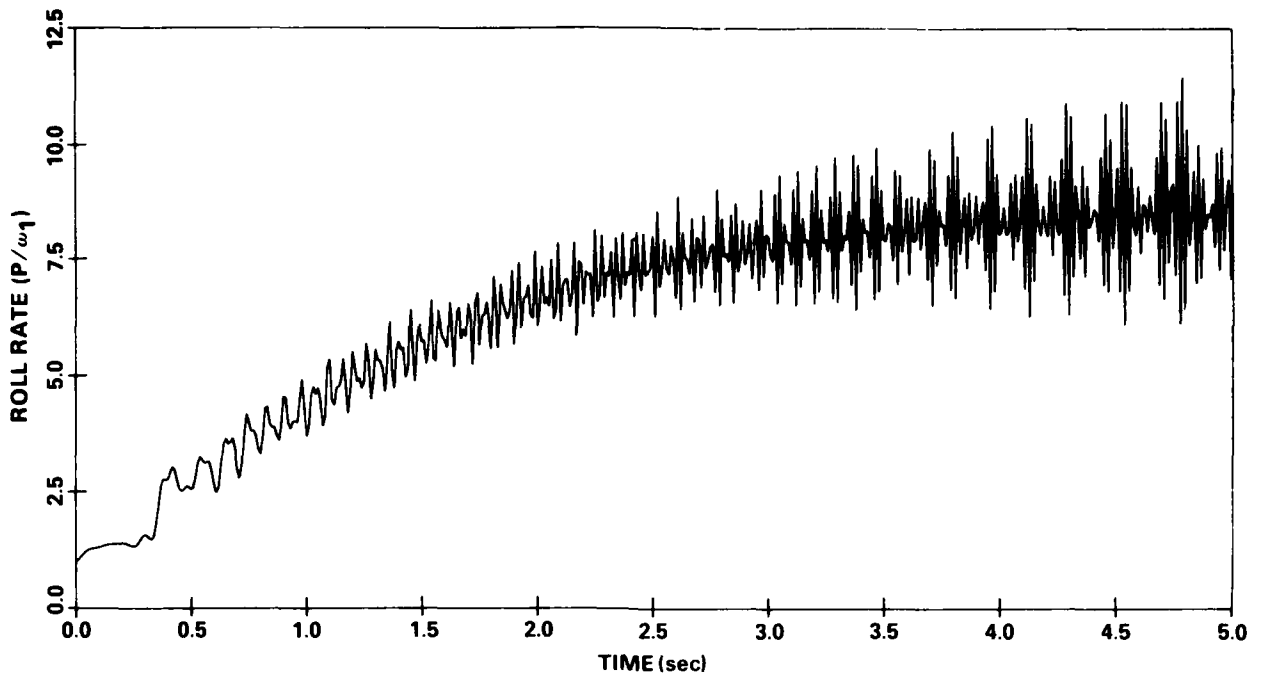


Figure 40. -Unstable Passage Through Resonance

CHAPTER VI

SUMMARY AND CONCLUSIONS

The free-flight angular motion of a symmetric cruciform missile, in the presence of nonlinear-roll-orientation-dependent aerodynamics has been treated in a manner amenable to deriving practical stability criteria. An aerodynamic force and moment system, consistent with arguments of rotational and reflectional symmetry, have been incorporated into the equations of motion. The method of multiple scales has been employed to obtain approximate expressions prescribing the missiles angular motion for the following conditions:

1. Free-flight yawing motion in the presence of nonlinear-roll-orientation-dependent aerodynamics with prescribed rolling motion
2. Free-flight rolling motion in the presence of linear damping and nonlinear induced roll moments
3. Aerodynamically coupled, free-flight yawing and rolling motion both away from, and in the neighborhood of resonant spin.

For the case of free-flight yawing motion with a priori rolling motion, an application of the method of multiple scales yields first-approximate solutions identical to those generated by the method of averaging. Critical roll rates are identified, and solutions valid in the vicinity of resonance are derived. Approximate solutions show good agreement with direct numerical solutions for moderate angles of attack and as such should provide useful stability criteria.

Nonlinear rolling motion with prescribed yawing motion was analyzed using a generalized version of the method of multiple scales. Singular roll rates of zero-spin, resonance, and one-half resonant spin were identified and solutions valid in the neighborhood of these roll rates derived. Comparisons with direct numerical integrations were accomplished by matching resonant and nonresonant solutions throughout the roll rate spectrum. Approximate solutions were shown to remain valid for moderate angles of attack below 30 degrees.

The complete problem of coupled nonlinear rolling and yawing motion was investigated and approximate solutions describing the motion were found to be simultaneous solutions of the prescribed roll and yaw cases. Solutions valid in the vicinity of resonance were derived and combined with small perturbation methods to derive useful stability criteria.

The above analyses have clearly shown the existence of resonance instabilities due solely to the inherent lack of complete axial symmetry introduced by the fin cruciform. Through the use of the derived approximate solutions, stability criteria may be used to investigate the frequency of occurrence or susceptibility of candidate configurations to resonance instabilities.

REFERENCES

1. J. D. Nicolaides, *Two Non-Linear Problems in the Flight Dynamics of Modern Ballistic Missiles*, IAS Report 59-17, 1959.
2. W. R. Chadwick, *Flight Dynamics of a Bomb With Cruciform Tail*, Journal of Spacecraft (June 1967).
3. T. A. Clare, *Resonance Instability for Finned Configurations Having Nonlinear Aerodynamic Properties*, Journal of Spacecraft and Rockets, Vol. 8, No. 3 (March 1971).
4. J. E. Brunk, *A Motion Theory for Sounding Rockets With Non-Linear Side and Magnus Moments*, presented at the AIAA Sounding Rocket Vehicle Technology Specialist Conference, Williamsburg, Va. (February 1967).
5. A. H. Nayfeh, *An Analysis of Asymmetric Rolling Bodies With Nonlinear Aerodynamics*, AIAA Journal, Vol. 10, No. 8 (August 1972).
6. C. H. Murphy, *Nonlinear Motion of a Missile With Slight Configurational Asymmetries*, presented at the AIAA Atmospheric Flight Mechanics Conference, Tullahoma, Tennessee (May 1970).
7. C. H. Murphy, *Response of an Asymmetric Missile to Spin Varying Through Resonance*, AIAA Journal, Vol. 9, No. 11 (November 1971).
8. C. H. Murphy, *Free Flight Motion of Symmetric Missiles*, BRL Report No. 1216, Aberdeen Proving Ground, Maryland (July 1963).
9. E. W. Reece, *Six Component Force Test of the TX-61 at Mach 0.7 to 2.5 With Varying Angles of Attack and Roll Angles*, SC-TM-65-575, Sandia Laboratories, Albuquerque, New Mexico (February 1966).
10. E. W. Reece, *Results of a Wind Tunnel Test to Determine the Effect of Roll Position on the Longitudinal Static Stability of the Tomahawk Rocket Configuration at Mach 7.3*, SC-TM-66-495, Sandia Laboratories, Albuquerque, New Mexico (October 1966).
11. F. J. Regan, V. L. Schermerhorn, and M. E. Falusi, *Roll-Induced Force and Moment Measurements of the M823 Research Store*, NOLTR 68-195, U. S. Naval Ordnance Laboratory, White Oak, Md. (November 1968).
12. C. G. Maple and J. L. Synge, *Aerodynamic Symmetry of Projectiles*, Quarterly of Applied Mathematics, Vol. VI, No. 4 (January 1949).
13. K. L. Neilson and J. L. Synge, *On the Motion of a Spinning Shell*, Quarterly of Applied Mathematics, Vol. IV, No. 3 (October 1946).
14. S. J. Zarodny, *Exercises on Maple-Synge Analysis of Consequences of Symmetry*, BRL Report No. 930, Aberdeen Proving Ground, Md. (February 1955).
15. T. R. Pepitone and I. D. Jacobson, "Resonant Behavior of a Symmetric Missile Having Roll Orientation-Dependent Aerodynamics," *Journal of Guidance and Control*, Vol. 1 (September-October 1978), pp. 335-339.

APPENDIX

MAPLE-SYNGE THEORY

The essence of the Maple-Syngé theory lies in its representation of the fluid forces and moments as power series expansions in the cross velocity components and in its arguments of the symmetry of these forces and moments under coordinate transformation.

For purposes of illustration, the derivation of the static forces and moments are considered here. For a more complete treatment, the reader is referred to Reference 12.

The complex transverse force and moment coefficient expansions, by the "aerodynamic hypothesis," may be written in the missile-fixed system in the complex angle of attack ξ , where

$$\xi = \frac{v + iw}{V} \quad (\text{A-1})$$

as

$$(C_y + iC_z) = \sum_{i,j} C_{ij} \xi^i \bar{\xi}^j \quad (\text{A-2})$$

and

$$(C_m + iC_n) = \sum_{k,l} C_{kl} \xi^k \bar{\xi}^l \quad (\text{A-3})$$

The scalar V is the magnitude of the total velocity and $(\bar{\quad})$ denotes complex conjugation. The coefficients C_{ij} , C_{kl} , are, in general, complex and may also be functions of spin, Mach number and Reynolds number.

The consequences of tetragonal symmetry may be realized by a consideration of the cross force and moment coefficient expansions in a new coordinate system (x, y_1, z_1) obtained by a 90° rotation about the x -axis. The rotational symmetry of the missile requires that the force and moment coefficients, as viewed in both systems must be related by

$$(C_{y_1} + iC_{z_1}) = i(C_y + iC_z) \quad (\text{A-4})$$

$$(C_{m_1} + iC_{n_1}) = i(C_m + iC_n) \quad (\text{A-5})$$

with

$$\xi_1 = i\xi \quad (\text{A-6})$$

and

$$\bar{\xi}_1 = -i\bar{\xi} \quad (\text{A-7})$$

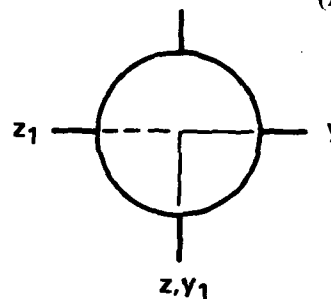


Figure A-1

Now assuming that the coefficients C_{ij} and $C_{k\ell}$ remain invariant, Equations (A-2) and (A-3) may be substituted into Equations (A-4) and (A-5) to obtain

$$\sum_{i,j} C_{ij}(\xi_1)^i(\bar{\xi}_1)^j = i \sum_{i,j} C_{ij}\xi^i\bar{\xi}^j \quad (\text{A-8})$$

$$\sum_{k,\ell} C_{k\ell}(\xi_1)^k(\bar{\xi}_1)^\ell = i \sum_{k,\ell} C_{k\ell}\xi^k\bar{\xi}^\ell \quad (\text{A-9})$$

Since the power series of Equations (A-8) and (A-9) must be equal term-by-term, consideration of Equations (A-6) and (A-7) requires that

$$i^{i-j-1} = 1 \quad (\text{A-10})$$

and

$$i^{k-\ell-1} = 1 \quad (\text{A-11})$$

or equivalently

$$i-j-1 = k-\ell-1 = 4N \quad (\text{A-12})$$

where N is an integer.

Therefore, the tetragonal symmetry requires that only those values of $i, j, k,$ and ℓ , in compliance with Equation (A-12), may occur in the cross force and moment expansions.

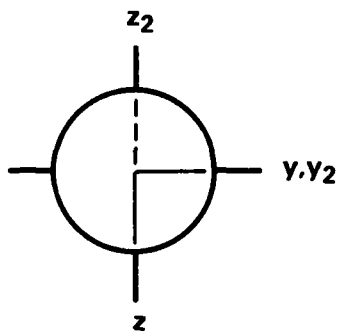


Figure A-2

The consequences of reflectional symmetry may be deduced by a consideration of the form of Equations (A-2) and (A-3) in a coordinate system, (x, y_2, z_2) obtained by reflection about the x - y plane. However, this reflection has changed the right-handed coordinate system (x, y, z) to a left-handed (x, y_2, z_2) system. Thus, the moment coefficient $(C_{m_2} + iC_{n_2})$ must be redefined in the (x, y_2, z_2) system. Maple and Syngé (A-2) adopt the definition that a rotation is positive if it corresponds to a cyclical rotation of the axes.

With this in mind, the force and moment expressions in the two systems are related by

$$(C_{y_2} + iC_{z_2}) = \overline{(C_y + iC_z)} \quad (\text{A-13})$$

and

$$(C_{m_2} + iC_{n_2}) = -\overline{(C_m + iC_n)} \quad (\text{A-14})$$

with

$$\xi_2 = \bar{\xi} \quad (\text{A-15})$$

Substitution of Equations (A-2) and (A-3) into Equations (A-13) and (A-14) yields

$$\sum_{i,j} C_{ij}(\xi_2)^i(\bar{\xi}_2)^j = \sum_{i,j} \bar{C}_{ij}(\bar{\xi})^i(\xi)^j \quad (\text{A-16})$$

$$\sum_{k,\ell} C_{m_{k\ell}}(\xi_2)^k(\bar{\xi}_2)^\ell = -\sum_{k,\ell} \bar{C}_{m_{k\ell}}(\bar{\xi})^k(\xi)^\ell \quad (\text{A-17})$$

Incorporation of Equation (A-15) leads to the conclusions

$$C_{ij} = \bar{C}_{ij} \quad (\text{A-18})$$

and

$$C_{m_{k\ell}} = -\bar{C}_{m_{k\ell}} \quad (\text{A-19})$$

Thus, reflectional symmetry requires the force coefficients C_{ij} to be real and the moment coefficients, $C_{m_{k\ell}}$ to be pure imaginaries.

In its most general form, then, the force and moment coefficient expansions for a symmetric cruciform missile may be written

$$(C_y + iC_z) = \sum_{N,j} C_{Nj}(\xi)^{j+4N}(\bar{\xi})^j \quad (\text{A-20})$$

$$(C_m + iC_n) = \sum_{N,\ell} C_{m_{N\ell}}(\xi)^{\ell+4N}(\bar{\xi})^\ell \quad (\text{A-21})$$

Expansions of Equations (A-20) and (A-21) for various values of N exhibit the form of the roll-orientation-dependent aerodynamics. For the case $N = 0$, Equations (A-20) and (A-21) yield

$$(C_y + iC_z)_0 = \sum_i C_{0j} \delta^{2j} \xi \quad (\text{A-22})$$

$$(C_m + iC_n)_0 = \sum_\ell C_{m_{0,\ell}} \delta^{2\ell} \xi \quad (\text{A-23})$$

where $\delta^2 = \xi\bar{\xi}$. Since all the terms in the expansions of Equations (A-22) and (A-23) are collinear with ξ , it is clear that the $N = 0$ terms are incapable of discerning the presence of the fins. However, consideration of the $N = \pm 1$ terms may be used to generate the roll orientation-dependent terms harmonic in 4γ . For $N = \pm 1$ the force and moment expansion becomes*

*Here the force coefficients (C's) have been replaced by the more conventional notation (C_N 's) with the subscript N denoting normal force.

$$(C_y + iC_z)_{N=\pm 1} = [C_{N-1,3} + C_{N-1,4}\delta^2 + C_{N-1,5}\delta^4 + \dots]\bar{\xi}^3 + [C_{N1,0} + C_{N1,1}\delta^2 + C_{N1,2}\delta^4 + \dots]\xi^5 \quad (\text{A-24})$$

$$(C_m + iC_n)_{N=\pm 1} = [C_{m-1,3} + C_{m-1,4}\delta^2 + C_{m-1,5}\delta^4 + \dots]\bar{\xi}^3 + [C_{m1,0} + C_{m1,1}\delta^2 + C_{m1,2}\delta^4 + \dots]\xi^5 \quad (\text{A-25})$$

Equations (A-24) and (A-25) may be put in standard form if the force and moment vectors are transformed to the nonrolling system through the transformations:

$$(C_{\tilde{y}} + iC_{\tilde{z}}) = e^{i\phi}(C_y + iC_z) \quad (\text{A-26})$$

$$(C_{\tilde{m}} + iC_{\tilde{n}}) = e^{i\phi}(C_m + iC_n) \quad (\text{A-27})$$

and

$$\tilde{\xi} = e^{i\phi}\xi \quad (\text{A-28})$$

with the result

$$(C_{\tilde{y}} + iC_{\tilde{z}})_{N=\pm 1} = [C_{N-1,3} + C_{N-1,3} + C_{N-1,4}\delta^2 + C_{N-1,5}\delta^4 + \dots]\delta^2 e^{-i4\gamma\tilde{\xi}} + [C_{N1,0} + C_{N1,1}\delta^2 + C_{N1,2}\delta^4 + \dots]\delta^4 e^{i4\gamma\tilde{\xi}} \quad (\text{A-29})$$

$$(C_{\tilde{m}} + iC_{\tilde{n}})_{N=\pm 1} = [C_{m-1,3} + C_{m-1,4}\delta^2 + C_{m-1,5}\delta^4 + \dots]\delta^2 e^{-i4\gamma\tilde{\xi}} + [C_{m1,0} + C_{m1,1}\delta^2 + C_{m1,2}\delta^4 + \dots]\delta^4 e^{i4\gamma\tilde{\xi}} \quad (\text{A-30})$$

where

$$\gamma = \theta - \phi \quad (\text{A-31})$$

Inspection of Equations (A-29) and (A-30) clearly reveals that the lowest-order terms capable of exhibiting roll orientation-dependence are third order in δ .

Combining the expansions for $N = 0, 1, -1$, static aerodynamic force, and moment coefficients to third order in δ may be obtained

$$(C_{\tilde{y}} + iC_{\tilde{z}}) = [C_{N_{0,0}} + C_{N_{0,1}}\delta^2 + C_{N_{-1,3}}\delta^2 e^{-i4\gamma} + \dots]\tilde{\xi} \quad (\text{A-32})$$

and

$$(C_{\tilde{m}} + iC_{\tilde{n}}) = [C_{m_{0,0}} + C_{m_{0,1}}\delta^2 + C_{m_{-1,3}}\delta^2 e^{-i4\gamma} + \dots]\tilde{\xi} \quad (\text{A-33})$$

Since all the $C_{m_{ij}}$'s are pure imaginary, Equations (A-32) and (A-33) may be written in the more conventional aerodynamic notation:

$$(C_{\tilde{y}} + iC_{\tilde{z}}) = [C_{N_{\alpha_0}} + C_{N_{\alpha^2}}\delta^2 + C_{N_{\gamma\delta^2}}\delta^2 e^{-i4\gamma} + \dots]\tilde{\xi} \quad (\text{A-34})$$

$$(C_{\tilde{m}} + iC_{\tilde{n}}) = i[C_{m_{\alpha_0}} + C_{m_{\alpha^2}}\delta^2 + C_{m_{\gamma\delta^2}}\delta^2 e^{-i4\gamma} + \dots]\tilde{\xi} \quad (\text{A-35})$$

Static aerodynamic expansions associated with the missile rolling motion may be derived using the same arguments of symmetry as in the case of missile transverse aerodynamics. The static roll moment coefficient, C_{ℓ} , is assumed to have a similar power series representation:

$$C_{\ell} = \sum_{ij} C_{ij} \xi^i \bar{\xi}^j \quad (\text{A-36})$$

where the C_{ij} are real. Following Maple-Synge symmetry arguments, if C_{ℓ} is viewed in the coordination system of Figure A-1, C_{ℓ} must remain invariant, or

$$C_{\ell} = C_{\ell_1}. \quad (\text{A-37})$$

Equation (A-37) may be expanded through the use of Equations (A-6), (A-7), and (A-36) to obtain

$$\sum_{k\ell} C_{k\ell}(\xi)^k(\bar{\xi})^{\ell} = \sum_{k\ell} C_{k\ell}(\xi_1)^k(\bar{\xi}_1)^{\ell} = \sum_{k\ell} C_{k\ell}(i)^{k-\ell}(\xi)^k(\bar{\xi})^{\ell}. \quad (\text{A-38})$$

Since the two series must be equal term by term, it is required that

$$i^{k-\ell} = 1 \quad (\text{A-39})$$

or equivalently

$$k - \ell = 4N \quad N = 0, \pm 1, \pm 2, \dots \quad (\text{A-40})$$

Thus the roll moment coefficient expansion must take the form

$$C_{\ell} = \sum_{N,\ell} C_{N\ell}(\xi)^{\ell+4N}(\bar{\xi})^{\ell} \quad N = 0, \pm 1, \pm 2, \dots \quad (\text{A-41})$$

Now Equation (A-41) may be rewritten in the slightly different form

$$C_{\ell} = \sum_{-N}^N \left\{ \left[\sum_{\ell=0}^N C_{N\ell} \delta^{2\ell} \right] \xi^{4N} \right\}. \quad (\text{A-42})$$

where $\delta^2 = \xi \bar{\xi}$. Now the terms with index $N = 0$ may be extracted from the summation to yield

$$C_{\ell} = \sum_{\ell=0}^{\infty} C_{0\ell} \delta^{2\ell} + \sum_{N=1}^{\infty} \sum_{\ell=0}^{\infty} \delta^{2\ell} [C_{N\ell} \xi^{4N} + C_{-N\ell} \bar{\xi}^{4N}], \quad (\text{A-43})$$

which is a statement of the linear superposition of the static roll driving terms, which are functions of yaw amplitude only, and the induced roll terms which are functions of ξ and its conjugate.

Expressing the complex angle of attack ξ in the missile fixed system as $\delta e^{i\gamma}$, the roll moment coefficient expansion may be written

$$C_{\ell} = \sum_{\ell=0}^{\infty} C_{0\ell} \delta^{2\ell} + \sum_{N=1}^{\infty} \delta^{4N} \sum_{\ell=0}^{\infty} \delta^{2\ell} \{C_{N\ell} e^{i4N\gamma} + C_{-N\ell} e^{-i4N\gamma}\} \quad (\text{A-44})$$

Since C_ℓ must remain a real quantity the condition

$$C_\ell = \bar{C}_\ell \quad (\text{A-45})$$

may be imposed and the two resulting infinite series equated term by term with the results

$$C_{0\ell} = \bar{C}_{-0\ell} \quad (\text{A-46})$$

and

$$\bar{C}_{N\ell} = C_{-N\ell} \quad (\text{A-47})$$

Incorporating Equations (A-46) and (A-47) into Equation (A-44) letting $C_{N\ell} = D_{N\ell}e^{i4\beta}$, the roll moment coefficient expansion yields:

$$C_\ell = \sum_{\ell=0}^{\infty} C_{0\ell}\delta^{2\ell} + \sum_{N=1}^{\infty} \delta^{4N} \left[2 \sum_{\ell=0}^{\infty} \delta^{2\ell} D_{N\ell} \cos 4(\beta + N\gamma) \right] \quad (\text{A-48})$$

where β is a constant angle related to the orientation of the fin cruciform in the missile-fixed coordinate system. If the cruciform is oriented coincident with the y-z axes (as is often the case) symmetry considerations require that the induced roll moment vanish at $\gamma = 0, \pi/2, \text{etc.}$, therefore

$$\beta = \pi/8 \quad (\text{A-49})$$

Thus the final form of the Maple-Syngé static roll moment coefficient expansion takes the form

$$C_\ell = \sum_{\ell=0}^{\infty} C_{0\ell}\delta^{2\ell} + \sum_{N=1}^{\infty} \delta^{4N} \sum_{\ell=0}^{\infty} \delta^{2\ell} B_{N\ell} \sin 4N\gamma \quad (\text{A-50})$$

The lowest-order terms in the expansion may be generated by a consideration of the terms associated with $\ell = 0, 1$ to obtain

$$C_\ell = C_{00} + C_{01}\delta^2 + \dots + B_{10}\delta^4 \sin 4\gamma + B_{11}\delta^6 \sin 4\gamma + B_{20}\delta^8 \sin 8\gamma + B_{21}\delta^{10} \sin 8\gamma + \dots \quad (\text{A-51})$$

or written in more conventional aerodynamic notation

$$\begin{aligned} C_\ell = & C_{\ell_0} + C_{\ell_{\delta^2}}\delta^2 + \dots + C_{\ell_{\gamma\delta^4}}\delta^4 \sin 4\gamma + C_{\ell_{\gamma\delta^6}}\delta^6 \sin 4\gamma \\ & + C_{\ell_{\gamma\delta^8}}\delta^8 \sin 8\gamma + C_{\ell_{\gamma\delta^{10}}}\delta^{10} \sin 8\gamma + \dots \end{aligned} \quad (\text{A-52})$$

DISTRIBUTION

Commander
Naval Air Systems Command
Washington, DC 20360
ATTN: AIR-320
AIR-320C
AIR-350
AIR-5301 (A. J. Besaha)
AIR-532

Commander
Naval Sea Systems Command
Washington, DC 20360
ATTN: SEA-62R (L. Pasiuk)

Commander
Naval Material Command
Washington, DC 20360
ATTN: CDR Denver Key
Technical Library

Office of Naval Research
800 North Quincy Street
Arlington, VA 22217
ATTN: Mr. D. Seigel
Dr. R. Whitehead
Technical Library

Commander
Naval Weapons Center
China Lake, CA 93555
ATTN: Code 3205 (L. Smith)
Code 3243 (R. E. Smith, S. Carter, E. N. Piper)
Code 3911 (R. D. Smith)
Code 3243 (K. Okauchi)
Technical Library

Commander
Naval Ordnance Station
Indian Head, MD 20640
ATTN: Mr. N. Sieden
Technical Library

Commandant of the Marine Corps
Headquarters, Marine Corps
Washington, DC 20380
ATTN: Technical Library

DISTRIBUTION (Continued)

Lockheed Missiles and Space Co.
PO Box 1103
Huntsville, AL 35807
ATTN: Mr. C. D. Andrews
Technical Library

Nielsen Engineering and Research, Inc.
510 Clyde Avenue
Mountain View, CA 94943
ATTN: Dr. M. J. Hensch
Mr. M. M. Briggs
Technical Library

Jones-Farley Associates
PO Box 695
Dahlgren, VA 22448
ATTN: Mr. H. Farley
Technical Library

The Raytheon Company
Missile Systems Division
Hartwell Road
Bedford, MA 01730
ATTN: Mr. D. P. Forsmo
Technical Library

Science Applications Inc.
2361 Jefferson Davis Highway
Arlington, VA 22217
ATTN: Mr. G. Gorman

Hughes Aircraft Company
Bldg. 262/C94
Canoga Park, CA 91304
ATTN: Mr. J. B. Harrisberger
Technical Library

Department of Aerospace & Mechanical Engineering
University of Notre Dame
Box 357
Notre Dame, IN 46556
ATTN: Dr. R. Nelson
Technical Library

Vought Corporation
Unit 2 - 55723
Box 225907
Dallas, TX 75265
ATTN: Mr. F. Prilliman
Technical Library

DISTRIBUTION (Continued)

Commander
U.S. Army Armament Research and Development Command
Dover, NJ 07801
ATTN: Technical Library

Commander
Ballistic Research Laboratory
Aberdeen Proving Ground, MD 21005
ATTN: Dr. C. H. Murphy
Technical Library

NASA Ames Research Center
Moffett Field, CA 94035
ATTN: Technical Library

NASA Langley Research Center
Langley Station
Hampton, VA 23365
ATTN: Mr. W. C. Sawyer
Mr. C. M. Jackson
Technical Library

Headquarters, NASA
Washington, DC 20546
ATTN: Technical Library

Director
Advanced Research Projects Agency
Department of Defense
Washington, DC 20305
ATTN: Technical Library

Applied Physics Laboratory
The Johns Hopkins University
Johns Hopkins Road
Laurel, MD 20810
ATTN: Mr. L. E. Tisserand
Technical Library

Martin-Marietta Aerospace
Orlando Division
PO Box 5837
Orlando, FL 32805
ATTN: Mr. G. F. Aiello (Mail Point 3)
Technical Library

DISTRIBUTION (Continued)

Superintendent
U.S. Naval Academy
Annapolis, MD 21402
ATTN: Prof. Gillerlain
LCDR Schlein
Technical Library

Superintendent
U.S. Naval Postgraduate School
Monterey, CA 95076
ATTN: Head, Department of Aeronautics
Technical Library

Commanding Officer
USAF Office of Scientific Research
Washington, DC 20330
ATTN: Technical Library

Commanding Officer
Wright Aeronautical Laboratory
Wright Patterson AFB, OH 45433
ATTN: Mr. G. Fleeman
Mr. M. Pinney
Dr. G. Kurylowich
Technical Library

Commanding Officer
Air Force Armament Laboratory
AFAFTL
Eglin AFB, FL 32542
ATTN: Dr. D. Daniel
Mr. K. Cobb
Technical Library

Superintendent
U.S. Air Force Academy
Colorado Springs, CO 80912
ATTN: Technical Library

Commander
U.S. Army Missile R&D Command
Redstone Arsenal
Huntsville, AL 35809
ATTN: Code DRDMI-TDK (R. Deep)
Technical Library

DISTRIBUTION (Continued)

Director, Development Center
Marine Corps Development and Education Command
Quantico, VA 22134
ATTN: Technical Library

Chief, Air Operations Division
Development Center
Marine Corps Development and Education Command
Quantico, VA 22134
ATTN: Technical Library

Director
Naval Research Laboratory
Washington, DC 20360
ATTN: Technical Library

Officer in Charge
U.S. Naval Scientific and Technical Intelligence Center
U.S. Naval Observatory
Washington, DC 20360
ATTN: Technical Library

Commander
Pacific Missile Test Center
Point Mugu, CA 93041
ATTN: Code 1244 (K. A. Larsen)
Technical Library

Commander
Naval Air Test Center
Patuxent River, MD 20670
ATTN: Technical Library

Commander
Naval Air Development Center
Warminster, PA 18974
ATTN: Technical Library

Commander
David W. Taylor Naval Ship Research & Development Center
Bethesda, MD 20084
ATTN: Code 1660 (R. M. Taylor)
Technical Library

DISTRIBUTION (Continued)

General Dynamics/Pomona Division
PO Box 2507
Pomona, CA 91766
ATTN: Dr. D. J. Trulin
Technical Library

Defense Technical Information Center
Cameron Station (12)
Alexandria, VA 22314

Library of Congress
Washington, DC 20540
ATTN: Gift and Exchange Division (4)

Defense Printing Service
Washington Navy Yard
Washington, DC 20374

Local:

E
E31 (GIDEP)
E41
F
F10
G
G10
G20
G204 (Chadwick)
G23 (Ohlmeyer)
G30
G41 (Fortunato)
K
K04
K10
K11
K11 (Daniels)
K20
K204
K21
K21 (Hardy, Katz, Solis, Weisel, Rutledge)
K21 (Pepitone) (10)
K22
K22 (Regan, Hannah, Brunsvold, Halupka)
K23
K24
K24 (Krumins, Yanta, Baltakis, Morrison)

DISTRIBUTION (Continued)

K30
K40
K50
N
N10
N20
N30
N40
N50
X210

(6)